# Assessing current and future spatiotemporal precipitation variability and trends over Uganda, East Africa based on CHIRPS and Regional Climate Models Datasets

Hamida Ngoma[1, 4], Wang Wen[1*], Moses Ojara[1, 3], Brian Ayugi[1,2]

[1]Key Laboratory of Meteorological Disaster, Ministry of Education (KLME)/Joint International Research Laboratory of Climate and Environment Change (ILCEC)/Collaborative Innovation Center on Forecast and Evaluation of Meteorological Disasters (CIC-FEMD), Nanjing, University of Information Science and Technology, Nanjing 210044, China

[2]Jiangsu Key Laboratory of Atmospheric Environment Monitoring and Pollution Control, Collaborative Innovation Center of Atmospheric Environment and Equipment Technology, School of Environmental Science and Engineering, Nanjing University of Information Science and Technology, Nanjing 210044, China

[3]Uganda National Meteorological Authority, Clement Hill Road, P.O. Box 7025 Kampala, Uganda

[4]Makerere University, Department of Geography, Geoinformatics and Climatic Sciences, P.O. Box 7062 Kampala Uganda

*Corresponding author: 001869@nuist.edu.cn

## Abstract

The lack of reliable rainfall projection records remains a major challenge to Uganda. In the advent of extreme wetness or drought events, reliable rainfall estimates for local planning and adaptation are essential. The present study used two main datasets to conduct a historical analysis from 1981 to 2019, coupled with future projections under representative concentration pathway (RCP 8.5) for the period 2020-2050. Historical analysis revealed bimodal annual rainfall pattern for March-May (MAM) and September-November (SON) gradients representing heavier to lighter rainfall events respectively over the study area. Investigation of recent trends in rainfall patterns revealed an upward trend from 2010 onwards in annual and seasonal rainfall. Moreover, results for future projections show wet conditions are projected to occur over the study area between the months of April/May and October. Contrarily, March is likely to experience a reduction in wet conditions. Mann-Kendall test employed to make future projections of rainfall depicted decreasing patterns during MAM season whilst increasing tendencies with strong shift was highlighted for SON season over the study region. Meanwhile, annual projections indicate huge variations with linear trends showing a marginal increase as compared to historical trends. Findings would serve as baseline print to propel further studies

 doi:10.20944/preprints202101.0037.v1

that could delve into impact analysis of drought extreme events which pose significant threats to the agricultural sector which is heavily reliant on rainfall.

**Keywords:** Rainfall, Trends analysis, Mann-Kendall test, CHIRPS, Rossby Centre regional Atmospheric model (RCA4), Uganda.

## 1. Introduction

Many African nations rely heavily on rainfall for agricultural activities, hydroelectric production and water supply for their day-to-day activities. A variability in rainfall occurrence (i.e., below normal leading to drought or above normal resulting to flood incidences) has far-reaching consequences on the economic stability of many regions. Thus, an accurate rainfall quantification remains a paramount process for sustainable development. Meanwhile, recent decades have been characterized by the emergence of extreme climatic events over many countries in both hemispheres, mainly due to global warming (Alexander et al. 2006; Seneviratne et al. 2013; Sillmann et al. 2013). Unprecedented changes in global climatic conditions have been induced by anthropogenic activities, resulting from an increase in the concentration of greenhouse gases (GHGs) in the atmosphere (IPCC 2013).

Presently, the outcome of several studies has shown developing countries would bear the unfortunate impacts of extreme weather events such as drought, floods, heatwaves, tropical cyclones, and wildfires as compared to mid-latitude and northern hemispheric nations (Seneviratne et al. 2012; Niang et al. 2014; Reliefweb 2020; Eckstein et al. 2020). Climate hazards would influence agricultural productivity (food security) in the sub-Saharan region (Parry et al. 2005; Schlenker and Lobell 2010). This threat could be further exacerbated by the increasing population, which is estimated to increase at approximately 4.8% per annum (FAO 2013). A recent report by FAO (2017) states about one-third of the human population is at risk of undernourishment in the East African region compared to other areas. This may be partly down to the declining tendency of 'long rains' which occurs between March and May (MAM) (Williams and Funk 2011; Lyon and Dewitt 2012; Liebmann et al. 2014). The situation is worsened by the uncertainties in future projections that continue to exhibit a 'paradox' scenario (Rowell et al. 2015). For instance, Tierney et al. (2015) shows future projection of MAM rainfall is likely to continue exhibiting observed negative trends while other studies (Rowell et al. 2015; Ongoma et al. 2018) reported increasing trends of precipitation towards the end of the twenty-first century. Such situations continue to pose confusion to all relevant stakeholders, thereby inhibiting progress planning and development policy.

Preprints (www.preprints.org) | NOT PEER-REVIEWED | Posted: 4 January 2021 doi:10.20944/preprints202101.0037.v1

Attributions to the uncertainties in the projections studies points a number of factors such as the systematic and unsystematic biases in model datasets or methods accounting for natural climate variability such as El Nino-Southern Oscillation or warming of tropical Oceans (Giannini et al. 2005; Eyring 2019). Other studies e.g. Christensen et al. (2008), Teutschbein and Seibert (2010) and Giorgi and Gutowski (2015), show that discrepancies in rainfall evaluation is sourced from the parameterization schemes in the global climate models (GCMs), such as those used in the fifth Coupling Modelling Inter-comparison Project (CMIP5) (Teutschbein and Seibert 2013). Thus, a number of recent studies (Nikulin et al. 2012; Endris et al. 2013) points to the need for consideration of employing dynamically downscaled regional climate models (RCMs), such as those from Coordinated Regional Climate Downscaling Experiment Program (CORDEX) for future climate projections. Recent studies have proven the better performance of RCMs in simulating the East African climate with the prospect of improvement in impact analysis (Endris et al. 2013; Osima et al. 2018; Ayugi et al. 2020a).

In Uganda, existing studies show average rainfall in the country has decreased by 12% (Ssentongo et al. 2018; Alex et al. 2019). The occurrence of single large-scale events like; droughts, floods, variable onset and offset of rainfall, long dry spells, are notable and is consistent with the prediction of IPCC (2014). An average annual rainfall range of 500.0 mm - 2500.0 mm is recorded in Uganda, whereas spatial variability in this range is large (Basalirwa 1995; McSweeney et al. 2010), as noted in other parts of East Africa (Hession and Moore 2011). With such changes in rainfall amount and trends, information on spatiotemporal changes would be valuable in developing preparedness measures as well as provision of early warning systems (Omondi et al. 2014). This is of particular importance as crop food production by local communities are directly affected leading to a reduction in the income of approximately 69% of Ugandan subsistence population (Gollin et al. 2016). Interestingly, despite the notable observations of changes in climate patterns over the study area, the existing ground-based datasets are sparsely distributed, hence, could not capture local changes in far remote regions with limited or no gauge stations (Kizza et al. 2009; Diem et al. 2014).

To improve prognosis and foster accurate forecast of climatic events, recent studies have gravitated towards RCMs and satellite-derived precipitation estimate (SPE) products as a way of detecting and projecting changes in climate incidences (Tian et al. 2010; Kidd et al. 2012; Nikulin et al. 2012). In addition, applications of SPE products in understanding extreme weather occurrences and analysis such as flooding or drought events have gained tremendous weight across the globe (Toté et al. 2015; Gebrechorkos et al. 2017). The present study sought to conduct an in-depth historical analysis of rainfall patterns over the study area using datasets

Preprints (www.preprints.org) | NOT PEER-REVIEWED | Posted: 4 January 2021 doi:10.20944/preprints202101.0037.v1

from Climate Hazard Group Infrared Precipitation with Station (CHIRPS) while future projection was evaluated using regional climate model obtained from multi-model ensemble from the Rossby Centre regional Atmospheric model (RCA4). We characterized recent changes in rainfall patterns and examined future projections using model datasets with fine spatial resolution. Subsequent sections of the present study constitute: Section 2 which entails description of the study area, datasets and methods. Section 3 presents the main results while section 4 elucidates summary, conclusion, and recommendations based on the findings.

## 2. Study Area, Data and Methods

### 2.1 Study Area

Uganda is located in East Africa. The geographical coordinates are within longitude 29° E to 35.2° E and latitude 4.5ºN to 1.5° S (**Figure 1**). Neighboring countries include Kenya, South Sudan, Democratic Republic of Congo, Tanzania and Rwanda. Complex topography and numerous physical features ranging from high mountainous ranges, large lakes and rivers, rich highlands to plain lands, characterize the study domain. For instance, Mount Elgon and Mount Rwenzori with approximately 4321m and 5109 m in height respectively are situated within the borders of the study area (Bowden and Semazzi 2007). Other geomorphological features within the study area are large water bodies such as Lake Victoria and river Nile which generate meso-scale circulation within the region (Indeje et al. 2001; Ogwang et al. 2014). The rainfall climatology is mostly influenced by the seasonal oscillation of Inter-Tropical Convergence Zone (ITCZ) (Nicholson 2018), monsoon winds and sub tropical anticyclones (Basalirwa 1995, Nicholson et al. 2017). Thus, most parts of the study area receive bimodal rainfall patterns with 'long rains' occurring in MAM whilst 'short rains' witnessed in September to November (SON) (Nsubuga et al. 2014; Ojara et al. 2020). This, however, results in a uni-modal pattern as the distance from the equator increases steadily. There is also another rainfall band mostly in the northern parts of the country occurring between June and August. This condition is often attributed to the influx of moist westerlies from Congo basin (Basalirwa 1995). On the other hand, the temperature climatology is mostly warm temperate during the year with peaks of highs, experienced during December-February (DJF) period and lows during June-August (JJA) period (Omondi et al. 2014). More details regarding the circulation patterns are well described in studies conducted by Nicholson et al. (2018) and Camberlin (2018).

Preprints (www.preprints.org) | NOT PEER-REVIEWED | Posted: 4 January 2021 doi:10.20944/preprints202101.0037.v1

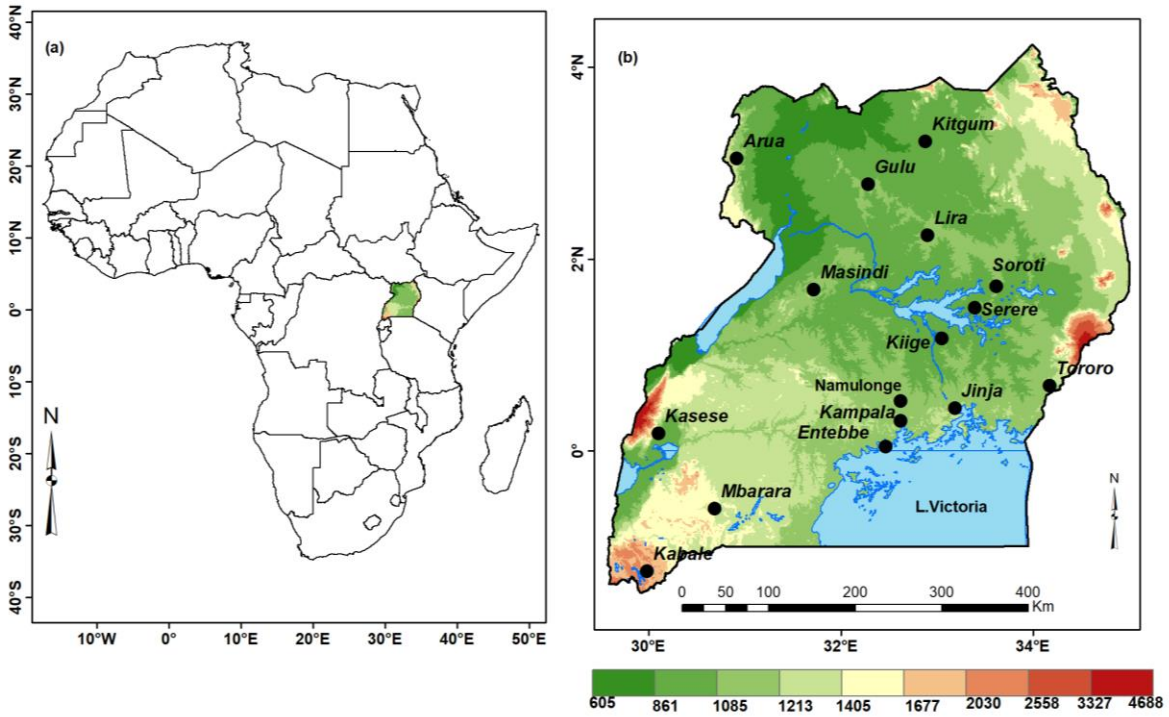


Figure 1. Location of Uganda along longitude 29° E – 35.2° E and latitude 1.5° S – 4.5° N in Africa (enclosed) (a). In addition, the figure shows the topography [m] of the study region, physical features and meteorological stations used (b).

## 2.2 Data

This study utilized monthly precipitation datasets obtained from Climate Hazard Group Infrared Precipitation with Station (CHIRPS.v2) (Funk et al. 2015), as well as Multi-model ensemble mean (MME) of five selected regional climate models (RCMs). The models were as follows: Model for Interdisciplinary Research on Climate (MIROC5), Commonwealth Scientific and Industrial Research Organization (CSIRO), Institute Pierre Simon Laplace Model CM5A-MR (IPSL-CM5A-MR), Max Planck Institute Earth System Model at base resolution (MPI-ESM-LR) and European community Earth-System (EC-EARTH). The listed RCMs simulations outputs were derived from the dynamical downscaling of CMIP5 GCMs using Rossby Centre regional Atmospheric model (RCA4), originally developed by the Swedish Meteorological and Hydrological Institute (SMHI) under the CORDEX initiative (Samuelsson et al. 2012). The RCA4 is a product of major enhancement on RCA3 based on model experimental design. Unden et al. (2002) and (Strandberg et al. 2014) gave detailed account regarding the physics of RCA4 model. The RCA4 simulations outputs are available on CORDEX-Africa domain at spatial resolution of ~ 50 km X 50 km and temporal coverage ranging from 1951-2005 for historical runs and projections from 2006-2100.

Preprints (www.preprints.org) | NOT PEER-REVIEWED | Posted: 4 January 2021 doi:10.20944/preprints202101.0037.v1

Both CHIRPS and MME datasets of five better performing RCMs were recently evaluated by inferring their performance over the study domain (Ayugi et al. 2019; Ayugi et al. 2020a). These models were appraised over the broader Greater Horn of Africa (GHA) against observed datasets using various scalar accuracy measures to assess their capability in reproducing fundamental precipitation characteristics over the study domain. The aforementioned studies used mean seasonal, annual, and inter-annual variations as a way of assessing their skillful simulation of precipitation over the region. Besides, a detailed statistical evaluation was employed to compare the model's performance. They included correlation coefficient (CC), mean bias error (MBE), and root mean square difference (RMSD), amongst the reanalysis and simulated precipitation cycle by the RCA4 models. Finally, the model's skill to simulate observed precipitation was tested using skill score, thereby identifying the five out of ten models evaluated in that study.

Consequently, the CHIRPS data covers the period 1981 to 2019. The CHIRPS datasets were validated against the available ground-based datasets to ascertain their performance on a monthly and annual time scale (**Figure 2; Table 2).** The MME of five RCMs was employed to delineate the future trends and variability of climatic features over the study domain. Historical analysis for validation on the performance over the study domain was performed during 1981-2005, while projections for future climatic trend and variability was assessed under high emission scenario of Representative Concentration Pathways (RCP 8.5) for 2020-2050 period. A summary of all model datasets used was shown in **Table 1,** indicating the type, source and resolution. All datasets were re-gridded using the bilinear interpolation technique to 0.5° x 0.5° spatial resolution in the present study. This was aimed to achieve uniform grids for analysis since the gridded datasets were of varying resolutions.

**Table 1 the** description of the Global Climate Models (GCMs) dynamically downscaled by RCA4 CORDEX.

| Institute | | Native horizontal grid increment | Abbreviated name | Reference |
|---|---|---|---|---|
| **1.** | Consortium of European research institution and researchers, Netherlands | 1.125°× 1.125° | EC-EARTH | Wazeleger et al. (2012) |
| **2.** | Institut Pierre-Simon Laplace, France | 3.75°×~ 1.895° | IPSL-CM5A-MR | Dufresne et al. (2012) |
| **3.** | National Institute for Environmental Studies, and Japan Agency for Marine-Earth Science and Technology (MIROC), Japan | ~1.4°×1.4° | MIROC5 | Watanabe et al. (2011) |
| **4.** | Commonwealth Scientific and Industrial Research Organization (Australia) | ~1.875°×1.875° | CSIRO-Mk3.6.0 | Rotstayn et al. (2009) |

Preprints (www.preprints.org) | NOT PEER-REVIEWED | Posted: 4 January 2021 doi:10.20944/preprints202101.0037.v1

| | | | | |
|---|---|---|---|---|
| **5.** | Max Planck Institute for Meteorology (Germany) | ~1.875°×1.875° | MPI-ESM-LR | Raddatz et al. (2007) |

178

179 **2.3 Methods**

180 **2.3.1 Validation of datasets**

181 Firstly, the present study validated the performance of both CHIRPS datasets and RCMs by
182 calculating *CC*, RMSD and MBE. These metrics have been employed by so many studies in
183 evaluating model simulation of climate variables (Wilks 2006; Chai and Draxler 2014; Ayugi
184 et al. 2020a). The mathematical formulas of the metrics employed are shown in Equations. 1 -
185 3:

186

187 $$CC = \frac{\sum_{k=1}^{n}(O_i - \overline{O_i})(M_i - \overline{M_i})}{\sqrt{\sum_{k=1}^{n}(O_i - \overline{O_i})^2 \sum_{k=1}^{n}(M_i - \overline{M_i})^2}} \quad (1)$$

188

189 $$RMSD = \sqrt{\frac{1}{N}\sum_{k=1}^{N}(M_i - O_i)^2} \quad (2)$$

190

191 $$MBE = \frac{1}{N}\sum_{k=1}^{N}(M_i - O_i) \quad (3)$$

192

193 Where *M* and *O* are the model simulated and observed values, respectively. *I* refers to the
194 simulated and observed pairs and *N* is the total number of such pairs being evaluated.
195 Taylor diagram and empirical cumulative distribution function (ECDF) were used to show the
196 comparison of the aforementioned datasets over the study area. Taylor diagram is a graphical
197 illustration showing similarity of two patterns in terms of their CC, centered RMSD, and the
198 amplitude of their variations (represented by the standard deviation) (Taylor 2001). All the
199 three metrics were presented on one plot as illustrated mathematically in Equation 4. The plot
200 was useful in evaluating multiple aspects of complex models or in gauging the relative skill of
201 many different models (IPCC 2001).

202 $$(E)^2 = {\sigma_m}^2 + {\sigma_o}^2 - 2\sigma_m\sigma_{Oo}C \quad (4)$$

203 Where E is centered RMSD
204 C is Correlation coefficient
205 $\sigma_m$ and $\sigma_o$ are standard deviation for the model and reference or observed datasets respectively.

Preprints (www.preprints.org) | NOT PEER-REVIEWED | Posted: 4 January 2021 doi:10.20944/preprints202101.0037.v1

A cumulative distribution F(x) can be defined as the proportion of observations lying below a certain value x as employed by Akinsanola (2017). The cumulative distribution of CHIRPS was compared with that of ground stations.

### 2.3.2 Spatiotemporal analysis

The study computed seasonal mean monthly rainfall by averaging three months total during the rainy seasons (i.e., MAM and SON). In addition, mean annual rainfall was derived by computing the average of all the monthly rainfall values over the study area. The evaluation of spatiotemporal patterns of rainfall for historical and future projections were conducted using anomaly test, thus, probability density function (PDF).

Anomaly is calculated from the Equation 5;

$$A = X - \bar{X} \tag{5}$$

### 2.3.3 Trend analysis

Precipitation trends are computed by fitting a linear model, using nonparametric Mann-Kendall test. The magnitude of change is computed using Sen's slope technique. The two main approaches were used to examine past and projected tendencies of precipitation. Firstly, we employed the Theil-Sen Slope technique to appraise the long duration tendencies. This method was used to evaluate the magnitude of the slope of the linear trend for a given data (Sen 1968). The method was considered to be effective since it is not influenced by any extreme distribution and does not entail any normal distribution of the residuals. Numerous studies have utilized this approach to examine the linear tendencies of hydroclimatic variables across various domains (Wang et al. 2018; Mumo et al. 2019; Ongoma et al. 2020). Mathematical expression explaining this approach is presented as follows:

$$\mathrm{SSE}_i = \frac{\mathrm{X_k} - \mathrm{X}_l}{\mathrm{k} - \mathrm{l}} \text{ for i} = 1, \ldots, \mathrm{n}, \tag{6}$$

where $i$ is the number of the time steps, $X_k$ and $X_l$ are the data points at point $k$ and $l$ respectively. In this case, $k$ must be greater than $l$. In case of only one datum in each period, then $n$ can be expressed as; $n = \frac{n(n-1)}{2}$. When there are multiple data in one or more-time periods, then $n < \frac{n(n-1)}{2}$. Where $n$ represents the time steps. The $n$ values of $SSE$ are arranged from smallest to largest. The Sen's slope estimator is calculated as;

$$\mathrm{Q_{med}} = \begin{cases} \mathrm{SSE}_{[(\mathrm{N}+1)/2]} & \text{when n is an odd number} \\ \dfrac{\mathrm{SSE}_{[\mathrm{N}/2]} + \mathrm{SSE}_{[(\mathrm{N}+1)/2]}}{2} & \text{when n is an even number} \end{cases} \tag{7}$$

Preprints (www.preprints.org) | NOT PEER-REVIEWED | Posted: 4 January 2021 doi:10.20944/preprints202101.0037.v1

The trend is indicated by the sign of the $Q_{med}$ while its value portrays the degree of the slope. The confidence interval of the $Q_{med}$ at certain probability is then obtained to check if the slope is statistically significant at zero. The confidence interval of the calculated gradient is shown in Equation (8) (Hollander et al. 2013):

$$C_\alpha = z_{1-a/2}\sqrt{S_v} \quad (8)$$

where the variance of $S_v$ is illustrated in Equation 11. $z_{1-a/2}$ is the tabulated value obtained from the t-table. According to Gilbert (1987), the lower and upper limits levels of the significant bands, $Q_{min}$, and $Q_{max}$, are $M_1{}^{th}$ largest and the $(M_2+1)^{th}$ largest of the $N$ ordered slope estimates. In this case, $M_1 = \frac{N-C_a}{2}$ and $M_2 = \frac{N+C_a}{2}$. In this study, the slope will be considered statistically significant at $(\alpha = 0.01)$ and if the two limits ($Q_{min}$ and $Q_{max}$) have same sign.

Secondly, the study further employed Mann-Kendall (MK); (Mann 1945; Kendall 1975) and Sequential Mann-Kendall (SQMK; Sneyer 1990) to determine the significance of the trend and possible abrupt changes in the timeseries. The MK test is a rank-based non-parametric method that checks the existence of trend in a time series against the null hypothesis of no trend. Several existing literatures have applied the MK test (Ongoma and Chen 2017; Ayugi et al. 2018; Ayugi et al. 2020b). Standardized MK trend statistics is calculated using the mathematical expression shown in equation 9:

$$S = \sum_{i=1}^{n-1}\sum_{j=i+1}^{n} \mathrm{sgn}(x_j - x_i) \quad (9)$$

where $x_i$ and $x_j$ are sequential data for the $i_{th}$ and $j_{th}$ terms, n is the sample size and

$$sgn(xj - xi) = \begin{cases} 1 \\ 0 \\ -1 \end{cases} \quad (10)$$

A hypothesis is set as follows; $H_0$ null hypothesis signifies no trend. Alternative hypothesis, $H_1$ indicates the presence of trend, either increasing or decreasing monotonic trend.

The variance was calculated using the following equation

$$Var(S) = \frac{n(n-1)(2n+5)}{18} \quad (11)$$

Preprints (www.preprints.org) | NOT PEER-REVIEWED | Posted: 4 January 2021 doi:10.20944/preprints202101.0037.v1

The probability associated with *S* and the sample size n is calculated to assess the significance of the trend. The scores of Z values also show the significance of the trend where the negative and positive scores of Z values denote downward and upward trends respectively. A two-tailed test, at a given α level of significance, $H_1$ is accepted if $|Z| > Z_{1-\alpha/2}$where $Z_{1-\alpha/2}$ is calculated from the standard normal distribution tables. The probability associated with MK and sample size *n* is computed to statistically quantify the significance of the trend. The normalized test statistic; Z is calculated using Eqn. (8);

$$Z = \frac{S-1}{\sqrt{Var(S)}} \quad if\ S > 0 \qquad (12)$$

$$=0 \text{if } S=0$$

$$= \frac{S+1}{\sqrt{Var(S)}} \quad \text{if } S<0$$

The trend is considered to be decreasing if Z is negative. For sequential Mann-Kendall (SQMK) test, forward sequential statistic: u (t) and backward sequential statistic u′(t) by Sneyers (1990) from the progressive analysis of MK test was used to investigate the change in trend of rainfall with time. In the computation, the test compared the relative magnitudes of data instead of the data values directly. In this case, u (t) is the standardized variable that has a unit standard deviation and a zero mean. The progressive MK values u (t) and u′(t), were calculated using the MK test for each data set, from the start to the end of the study period. In the plot of sequential MK, the confidence limits of the standard normal Z values are at α =5%. The upper and lower confidence limits therefore correspond to +1.96 and -1.96, respectively. A significant trend is noted if the progressive MK values cross either confidence limit lines at the 5% significance level.

## 3.0 Results and Discussions

### *3.1 Validation of datasets*

Figure 2 presents results obtained from the validation analysis of CHIRPS.v2 against in-situ datasets based on monthly distribution and annual cycle during the study period. These were derived from sixteen available ground-based datasets distributed across the country as shown in Figure 1**.** A summary of statistical metrics detailing the models' performance against observed datasets is shown in Table 2**.** Our results demonstrate that CHIRPS.v2 can reliably reproduce rainfall climatology over the study area. There is a strong agreement between CHIRPS datasets and ground-based on monthly distribution, with ECDF showing homogeneous patterns as observed along with the frequency distribution. Moreover, the CHIRPS products captured the annual cycle's bimodal patterns and seasonal peaks, as observed

Preprints (www.preprints.org) | NOT PEER-REVIEWED | Posted: 4 January 2021 doi:10.20944/preprints202101.0037.v1

using in-situ datasets **(**Figure 2b and Table 1**).** However, a slight overestimation was observed in April when the study region experienced the highest rainfall amount. Interestingly, the month of October and November depicted an underestimation of ground-based data by CHIRPS.v2.

Despite the reliability of CHIRPS.v2 in reproducing rainfall information, contrary performance was noted at Kitgum station. The CHIRPS.v2 showed a weak correlation (CC = 0.12) and high amplitude with RMSD = 179.11 mm/month and Bias = 39.58 **(**Table 2**).** This calls for further investigation of the observed outlier performance on this particular station. Overall, the CHIRPS datasets can be employed as an alternative to in-situ datasets in a region characterized by scarcity of ground-based datasets for a timely exploration of ever-increasing climate extremes.

**Table 2.** Annual statistical parameters obtained from the validation of ground-based vs remotely sensed rainfall CHIRPS.v2 datasets over Uganda during 1981-2017

| **Station** | Statistical metrics | | |
|---|---|---|---|
| | Correlation | RMSD | Bias |
| Arua | 0.76 | 52.79 | 5.57 |
| Entebe | 0.67 | 78.49 | 30.51 |
| Gulu | 0.85 | 44.84 | -0.45 |
| Jinja | 0.74 | 45.26 | -1.67 |
| Kabale | 0.78 | 34.46 | -0.96 |
| Kampala | 0.59 | 65.42 | 9.98 |
| Kasese | 0.78 | 32.83 | -4.41 |
| Kiige | 0.69 | 57.64 | 4.34 |
| Kitgum | 0.12 | 179.11 | 39.58 |
| Lira | 0.82 | 46.86 | 2.22 |
| Masindi | 0.72 | 50.3 | 1.04 |
| Mbarara | 0.77 | 34.91 | 4.46 |
| Namulonge | 0.65 | 48 | -11.56 |
| Serere | 0.49 | 73.39 | -3.2 |
| Soroti | 0.78 | 49.8 | -3.69 |
| Tororo | 0.75 | 50.69 | -4.58 |

Furthermore, this study sought to validate the performance of the better performing RCA4 model as recommended in a recent study (Ayugi et al. 2020a) against the "observed" CHIRPS.v2 datasets over Uganda during 1981-2005. Models were evaluated using robust statistical metrics such as CC, SD, RMSD, and MBE. Figure 3 shows the results of the performance of RCA4 models against the CHIRPS.v2 datasets. It demonstrated previous assessment's substantial similarity to few existing ground-based datasets over the study domain. The validation of the MME displays relatively better performance over the study

Preprints (www.preprints.org) | NOT PEER-REVIEWED | Posted: 4 January 2021 doi:10.20944/preprints202101.0037.v1

region. For instance, the correlation coefficient shows 0.9 with CHIRPS.v2, while RMSD depicts a low amplitude of < 50 %. Moreover, a relatively low standard deviation (about 0.65 mm/month) is simulated against the observed value of 1.0 mm/month. Therefore, the analysis elucidates the multi-model ensemble application for rainfall projections and impact analysis over the study area.

The results for CHIRPS and RCMs validation over the study region agree with many evaluative studies. For instance, the reliability of CHIRPS in reproducing regional rainfall information as compared to other satellite datasets across many regions in the sub-Saharan equatorial region as affirmed in various studies (e.g., Diem et al. 2014 2019b; Gebrechorkos et al. 2017; Kimani et al. 2017; Nicholson et al. 2019; Ayugi et al. 2019). It should be noted that the study area experiences heavy rains for MAM, and short rains are received for SON (Kizza et al. 2009; Ogwang et al. 2014; Gamoyo et al. 2015). The bimodal pattern is mostly influenced by the oscillation of Intertropical Convergence Zone (ITCZ) (Nicholson 2018; Yang et al. 2015; Nicholson et al. 2018).

Simultaneously, other studies have also substantiated that RCMs can generate high-resolution projections of climate events in many parts of the world as compared to Global Climate Models (GCMs) (Kidd et al. 2012; Nikulin et al. 2012). Recent evaluative studies on the performance of RCMs over the Greater Horn of Africa (GHA) identified the robust performance of RCMs derived from the Rossby Centre regional Atmospheric Model (RCA4) (Endris et al. 2013; Kisembe et al. 2019; Ayugi et al. 2020a). The validation of model performance over the study area reaffirms the trustworthiness and reliability of the RCMs in projecting the possible future changes amid climate change and global warming. Thus, this study employs the MME of the five models in the projection of precipitation change using the representative concentration pathways, proposed by Riahi et al. (2007).

Preprints (www.preprints.org) | NOT PEER-REVIEWED | Posted: 4 January 2021 doi:10.20944/preprints202101.0037.v1

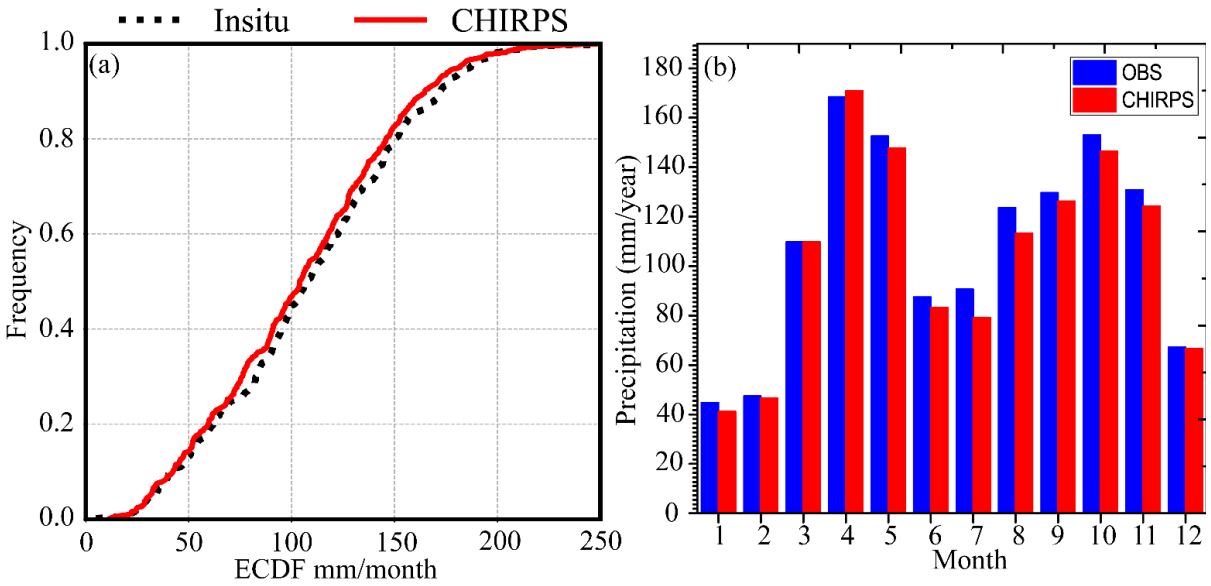


Figure 2. Comparison of CHIRPS.v2 against in-situ datasets based on (a) monthly distribution presented using the ECDF plots for the period 1981-2017 over Uganda. The second plot; (b) shows the annual cycle of precipitation products during the study period derived from sixteen available ground-based datasets distributed across the country as shown in Fig. 1

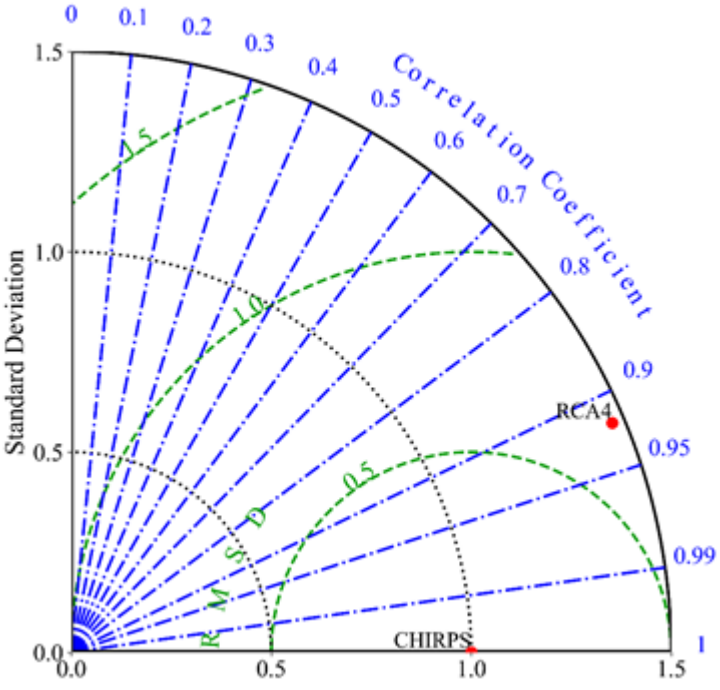


Figure 3. Taylor diagram showing the validation of RCA4 model against the "observed" CHIRPS.v2 datasets over Uganda during 1981-2005. The statistical metrics computed entailed correlation coefficient, standard deviation, root mean square difference and bias.

*3.2 Spatiotemporal variability of annual and seasonal rainfall*

Preprints (www.preprints.org) | NOT PEER-REVIEWED | Posted: 4 January 2021 doi:10.20944/preprints202101.0037.v1

This analysis aimed to show the spatial and temporal patterns of rainfall change over Uganda during the recent period 1981 – 2019. The results are depicted in Figures 4 and 5, respectively. Figure. 4 shows an overview of the annual precipitation cycle and the rate of change per year over Uganda based on CHIRPS.v2 datasets for 1981-2019. It is apparent from the figure that the study area experiences bimodal rainfall patterns with a strong gradient of rainfall experienced during MAM period over the years along with the second rainfall band occurring during SON. The mean rainfall for MAM (SON) is 139.20 mm/month (125.71 mm/month). The results further illustrate that the study area received less rainfall of < 48 mm/month during the DJF season, while a substantial amount of rainfall (107 mm/month) is noted during the JJA period. Remarkably, the yearly variation shows that the year 2012 recorded the highest amount of rainfall, whereas the least amount was noted in the year 2009. The observed anomalies depict a period of dryness (wetness) over the study area. To understand the recent trends experienced over the given period, we employed Theil Sen Slope Estimator to compute the trends. Findings for the rate of change are presented in Figure 4b. As shown in the figure above, the results display a significant positive increase in October at 0.62 mm/year, while January and July depicted a negative insignificant decreasing pattern of -0.178 mm/year (-0.311) mm/year, respectively.

For seasonal tendencies, the MAM season shows a decreasing pattern compared to SON, which is considered a 'short rainy' season over the study region. Further analysis of the spatial distribution of seasonal rainfall (mm) and their respective probability density function (PDF) distribution over Uganda based on CHIRPS.v2 datasets for the period 1981 – 2019 is shown in Figure 5. Figure 5a shows spatial patterns of MAM rainfall, while SON rains are presented in Figure 5b. MAM receives more rainfall distribution compared to SON. Moreover, southern and eastern parts of the region experience a higher magnitude of rainfall, while the northeast depicts less precipitation amount of ≤ 50 mm/month. The rainfall amounts over the northeastern zone are more pronounced during SON, with larger parts of the study area receiving fewer rainfall amounts than MAM season. Despite the higher rainfall amount experienced during MAM season, analysis of PDF that examines the relative likelihood in the distribution of variable from the mean shows that SON is likely to shift from negative to positive patterns. The results presented provide information on how the region's rainfall has varied both in time and space.

Numerous existing studies have attempted to establish an explanation of monthly variations, the trends, and mechanisms regulating the observed patterns. For instance, the seasonal variability of rainfall is regulated mainly from the complex interaction of weather

Preprints (www.preprints.org) | NOT PEER-REVIEWED | Posted: 4 January 2021 doi:10.20944/preprints202101.0037.v1

systems such as; the bi-annual oscillation of ITCZ from North to South, the tropospheric systems of Quasi-biennial Oscillation (QBO), large-scale monsoon winds, and subtropical anticyclones (Mutai et al. 2000; Nsubuga et al. 2011). The ITCZ has a larger influence than the listed underlying mechanisms of seasonal rainfall patterns (Nicholson 2018). Meanwhile, the increasing amount of rainfall during the period of JJA, which was considered as the local dry season, is attributed to moist westerlies originating from the Congo basin resulting to enhanced rain during this season in the north and southwest when other parts of the country are cold and dry (Mchugh 2004; Kizza et al. 2009). On the other hand, Lake Victoria's lake/land breeze plays a significant role in driving the rainfall being experienced during the dry season of DJF (Nsubuga and Rautenbach 2017). The present study's findings correspond to past studies that noted the observed climatology of enhanced rainfall during JJA season (Nsubuga et al. 2014; Yang et al. 2015).

On the linear trend analysis, other existing studies equally noted a declining trend in rainfall during the local wet season of MAM (Funk et al. 2005; Lyon and Dewitt 2012; Liebmann et al. 2014). The season mentioned above is considered as the main growing season for agricultural activities that support 70% of the local economy (McSweeney et al. 2010; Ojara et al. 2020). This decrease would influence food security and livelihoods of the people. In the meantime, the spatial patterns of rainfall that depicted a higher rainfall amount during MAM season over southern and eastern parts could be attributed to the presence of large water bodies, i.e., Lake Victoria and complex geomorphology situated over the regions that receive the highest amount of rainfall (Basalirwa 1995; Indeje et al. 2001; Ogwang et al. 2014). The presence of high elevation along the eastern region produces leeward rain shadows and block the passage of rain-bearing disturbances in other areas (Ogwang et al. 2014). On the other hand, the northeast locale is characterized by arid and semi-arid lands (ASALs) with scarce vegetation cover, low precipitation events, high evapotranspiration, strong radiation, and high wind patterns throughout the year. Such factors result to dry anomaly, which significantly impact on community livelihoods and other ecosystem processes. Overall, the MAM season is mainly regulated by a combination of mesospheric features and atmospheric circulation, thereby contributing to higher rainfall amount observed as compared to the SON season (Yin and Nicholson 2002). The PDF analysis depicted changes in the shift for seasonal rainfall distribution has been attributed to the alteration of Walker circulation anomalies due to intense warming of Sea surface temperature (SST) along the western Indian Ocean (Lyon and Dewitt 2012). The implication of the changes in the seasonal rains is likely to impact farmers'

Preprints (www.preprints.org) | NOT PEER-REVIEWED | Posted: 4 January 2021 doi:10.20944/preprints202101.0037.v1

uncertainties regarding crop growing seasons, which predominantly have been observed for MAM season (Matthew et al. 2015; Adhikari et al. 2015).

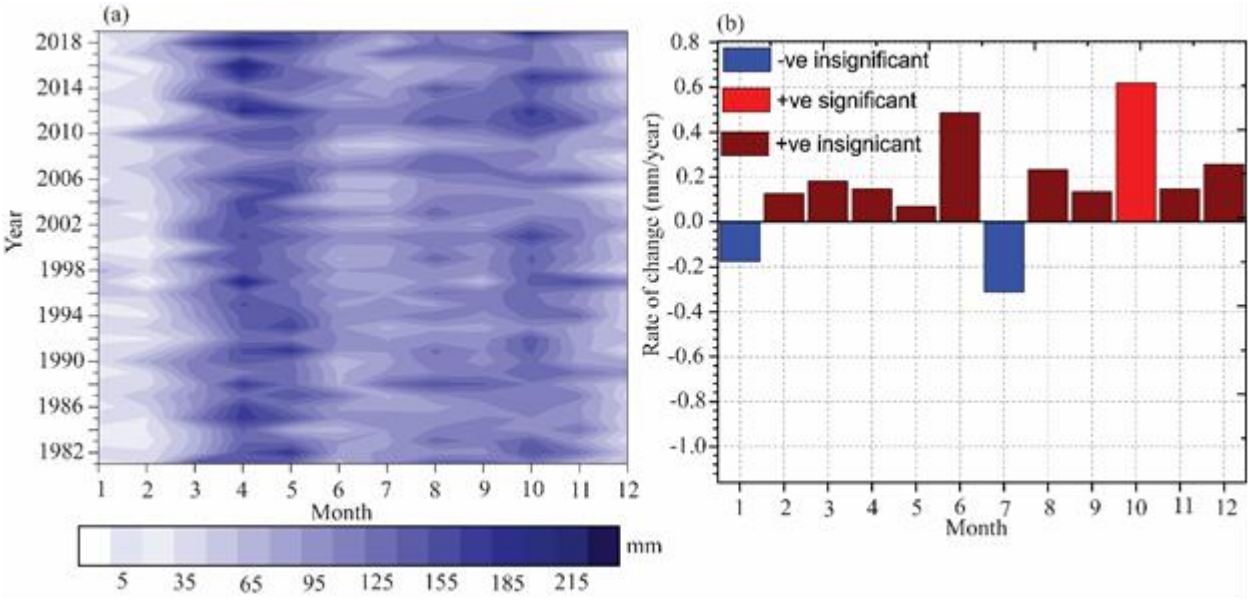


Figure 4. Yearly/monthly evolution of annual precipitation cycle and the rate of change per year over Uganda based on CHIRPS.v2 datasets for the period 1981-2019.

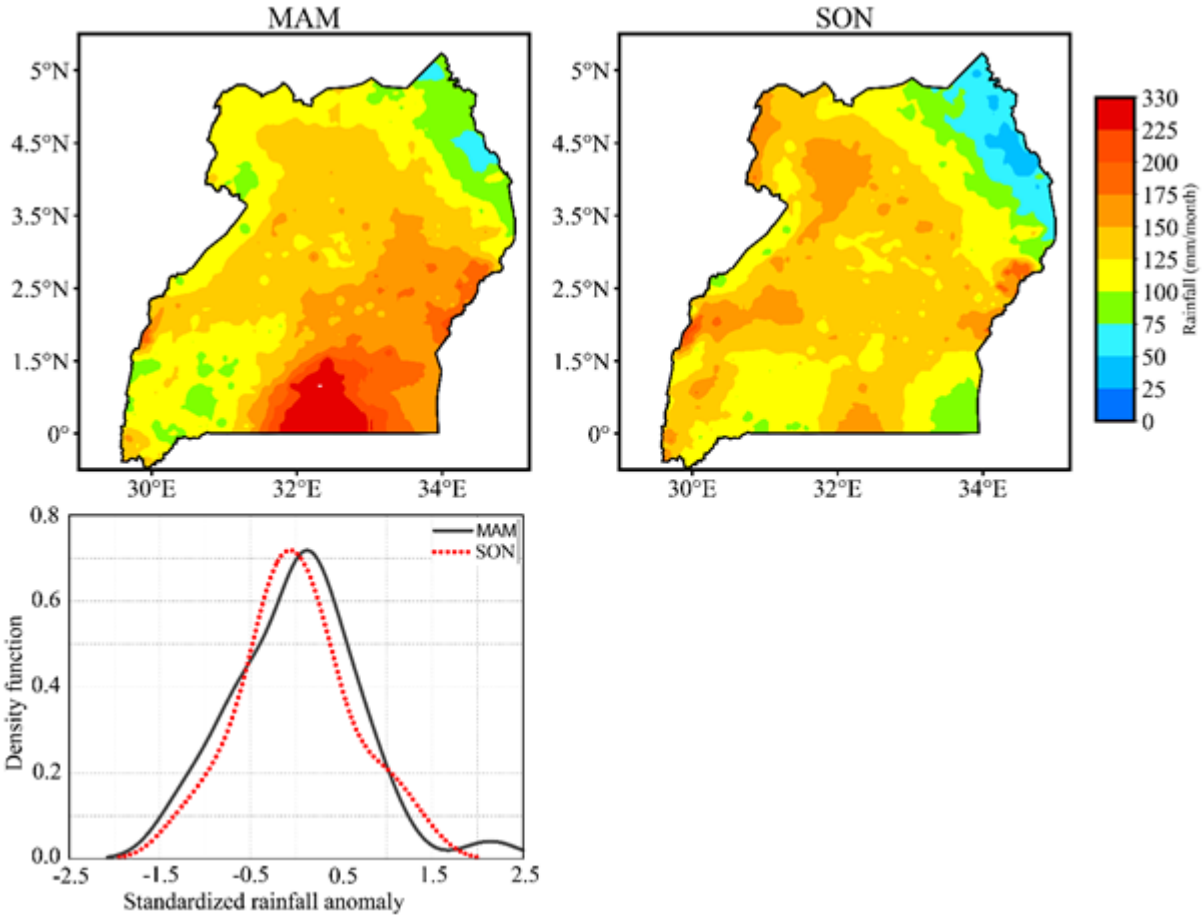

Preprints (www.preprints.org) | NOT PEER-REVIEWED | Posted: 4 January 2021 doi:10.20944/preprints202101.0037.v1

Figure 5. Seasonal mean monthly rainfall (mm) and their respective probability density function (PDF) distribution over Uganda based on CHIRPS.v2 datasets for the period 1981-2019; March-May (left), and September-November (right).

*3.3 Interannual variability of seasonal and annual rainfall*

Analysis of rainfall anomalies for seasons over the study region during the1981 – 2019 period based on CHIRPS.v2 datasets is presented in Figure 6. Examining the interannual variability of rainfall aids in the understanding of the main factors controlling the interannual variations. Typical wet and dry years were identified following Makkonen's (2006) recommendations on exceeding the standard deviation of +1/-1. The results show substantial variability on interannual rainfall patterns over the study domain. For instance, the local wet season for MAM highlights wet and dry patterns with 23 years experiencing wet anomalies while 15 years had incidences of dry anomalies. On the other hand, SON shows an equal number of years of wet and dry events although annual records depicted 55 % (21/38 years) of the total years with a positive standardized anomaly. Notable wet years during the rainy seasons and annually were as follows: 2011 and 2012, whereas dry years were observed during 2008 and 2009.

Further analysis of rainfall decadal change is shown in Figures 7 and 8. A decadal study reveals low-frequency phenomena modulating climatic regimes and precipitation variability (White and Tourre 2003). In this study, we analyzed decadal to show spatial variations of rainfall and to identify the years associated with climatic phenomenon regulating the interannual and interdecadal variability. The spatial anomalies were calculated based on CHIRPS datasets over the last four decades, thus, 1981 - 1990; 1991 – 2000; 2001 – 2010; and 2011 – 2019. The summary of the rate of change per decade is highlighted in Table 3. From the analysis based on rainfall decadal anomalies, it is apparent that varying tendencies were noted from one decade to another across various time scales. For instance, the study region witnessed a pronounced decreasing trend during MAM seasons through the last decade (2011 – 2019) though SON showed a decreasing trend during the first two decades (1981 – 1990 and 1991 – 2000) coupled with a recovery afterwards. Moreso, MAM depicted distinct wetting trends covering most parts of the study area during the first three decades (i.e., 1981 - 1990, 1991 - 2000, and 2001– 2010) although dry trends were observed in 2011 – 2019 (Figure 7). The SON rains (Figure 8) exhibited a reduction trend in the first two decades (1981 – 1990 and 1991 – 2000), followed by an increase in the last decades (2001 – 2010 and 2011 – 2019), probably reflecting an increased November rainfall over broader study locale (Spinage 2012). Overall, the observed patterns show a reversal in rainfall patterns over the study region with

Preprints (www.preprints.org) | NOT PEER-REVIEWED | Posted: 4 January 2021 doi:10.20944/preprints202101.0037.v1

enhanced rainfall occurrence during the short rain season whereas reduction was witnessed during the long rain season.

The result from the inter-annual variation analysis shows high spatiotemporal variability, which coincides with the anomalies in remote forcing events. For example, the primary controlling mechanism influencing the observed interannual variations high/low rainfall events have been linked to the dipole reversal of atmospheric circulation and Indian Ocean sea surface temperatures (Saji et al. 1999). The rains are moderated by weather phenomena such as El Niño Southern Oscillation (ENSO) (Indeje et al. 2000; Ntale and Gan 2003) and the Indian Ocean Dipole (IOD) (Behera et al. 2006). The El Niño Southern Oscillation (ENSO) phenomena are strongly associated with the inter-annual variability of rainfall in this region (Indeje et al. 2000). This is reflected in the present study as years with El Niño events such as 2010 and 2012 were recorded as wet years whereas La Nina events coincided with dry years such as 1984, 1992, and 2008. The inter-annual variability of SON rains is mostly attributed to ENSO and IOD influence.

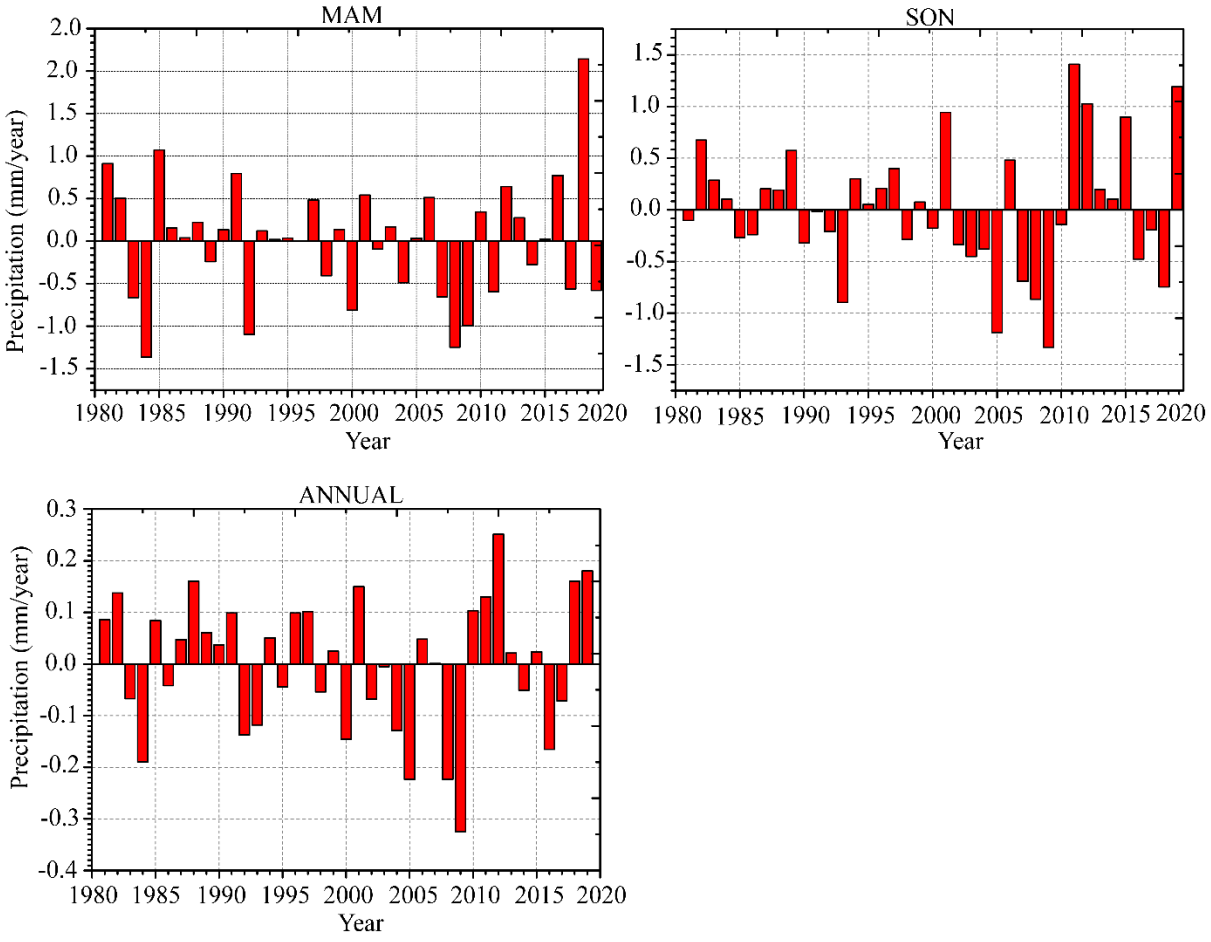


Figure 6. Precipitation anomalies for MAM, SON, and Annual occurrence over Uganda during 1981-2019 based on CHIRPS.v2 datasets

Preprints (www.preprints.org) | NOT PEER-REVIEWED | Posted: 4 January 2021 doi:10.20944/preprints202101.0037.v1

The decadal anomalies revealed an increase in anomalous events that have been mostly associated with positive Indian Ocean Dipole instead of the teleconnection patterns across the Pacific Ocean (Behera et al. 2006; Muhati et al. 2007). The increasing positive IOD phase results from the heightened warming of the Western Indian Ocean, which alters the changes in Walker Circulation (Behera et al. 2006; Ogwang et al. 2015). Several studies have reported that SON rainfall is mostly influenced by the changes in ENSO and IOD (Saji and Yamagata 2003; Manatsa et al. 2012). On the other hand, MAM rains occurred as a result of three main drivers, the Indian Ocean SST, the seasonal amplitude of the Madden Julian Oscillation (MJO), and the phase of the quasi-biennial oscillation (QBO) (Vellinga and Milton 2018; MacLeod 2019). The observed decline in MAM rainfall in the region has been prominently analyzed and discussed (Funk et al. 2008; Rowell et al. 2015). Williams and Funk (2011) attributed the continuous drying over the EA region to an anthropogenic-forced relatively enhanced warming of Indian Ocean SSTs, which extends the warm pool and Walker circulation westward, leading to a subsidence anomaly causing the drying effects. The observed trends have already affected many communities that rely on rainfall for their socio-economic activities. (Funk et al. 2008).

The local impact of the interannual variability observed had immense impact on the livelihoods of people. For example, the periods of negative anomalies have resulted in droughts that have been identified to align with ENSO-related anomalies. The impact of drought has remarkably altered water resources, ecosystem balance, and impacted on agricultural activities. Previous work by Apuuli et al. (2000) noted how people were displaced during drought years with exorbitant food prices across the study area. Climate anomalies resulting in dry conditions have impacted Uganda with average damage over the past decade of about $ 237 USD (GOU 2015). Such impacts enhanced increasing calls for close monitoring of climate systems in order to design appropriate policies, aimed at preparing communities to cushion themselves against direct and indirect impacts.

**Table 3**. Decadal change in precipitation over Uganda during 1981-2019 based on CHIRPS.v2 datasets

| | | 1981-1990 | 1991-2000 | 2001-2010 | 2011-2019 |
|---|---|---|---|---|---|
| **MAM** | Mean (mm) | 138.33 | 136.61 | 136.12 | 146.45 |
| | Rate (mm /year) | -1.593 | -0.701 | -2.725 | 0.4337 |
| **SON** | Mean (mm) | 122.94 | 123.07 | 116.67 | 139.58 |
| | Rate (mm /year) | -0.028 | 0.644 | -1.8 | -4.58 |
| **Annual** | Mean (mm) | 103.77 | 103.72 | 102.27 | 111.87 |
| | Rate (mm/year) | 0.3303 | 0.0084 | -1.42 | -0.1733 |

Preprints (www.preprints.org) | NOT PEER-REVIEWED | Posted: 4 January 2021 doi:10.20944/preprints202101.0037.v1

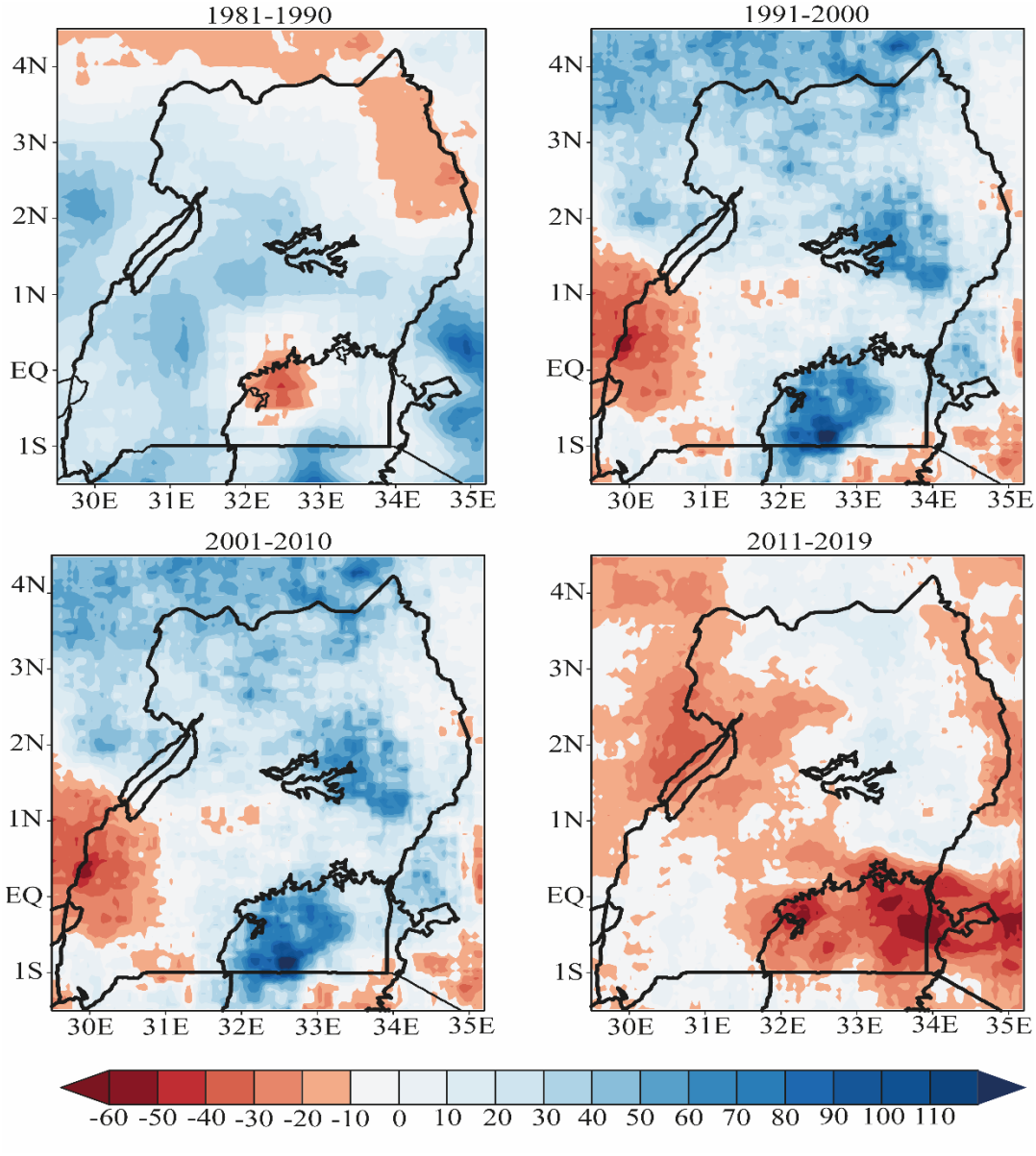


503

504 Figure 7. Spatial decadal precipitation anomalies (mm) for MAM over Uganda based on
505 CHIRPS.v2 datasets for the period 1981-2019.

Preprints (www.preprints.org) | NOT PEER-REVIEWED | Posted: 4 January 2021 doi:10.20944/preprints202101.0037.v1

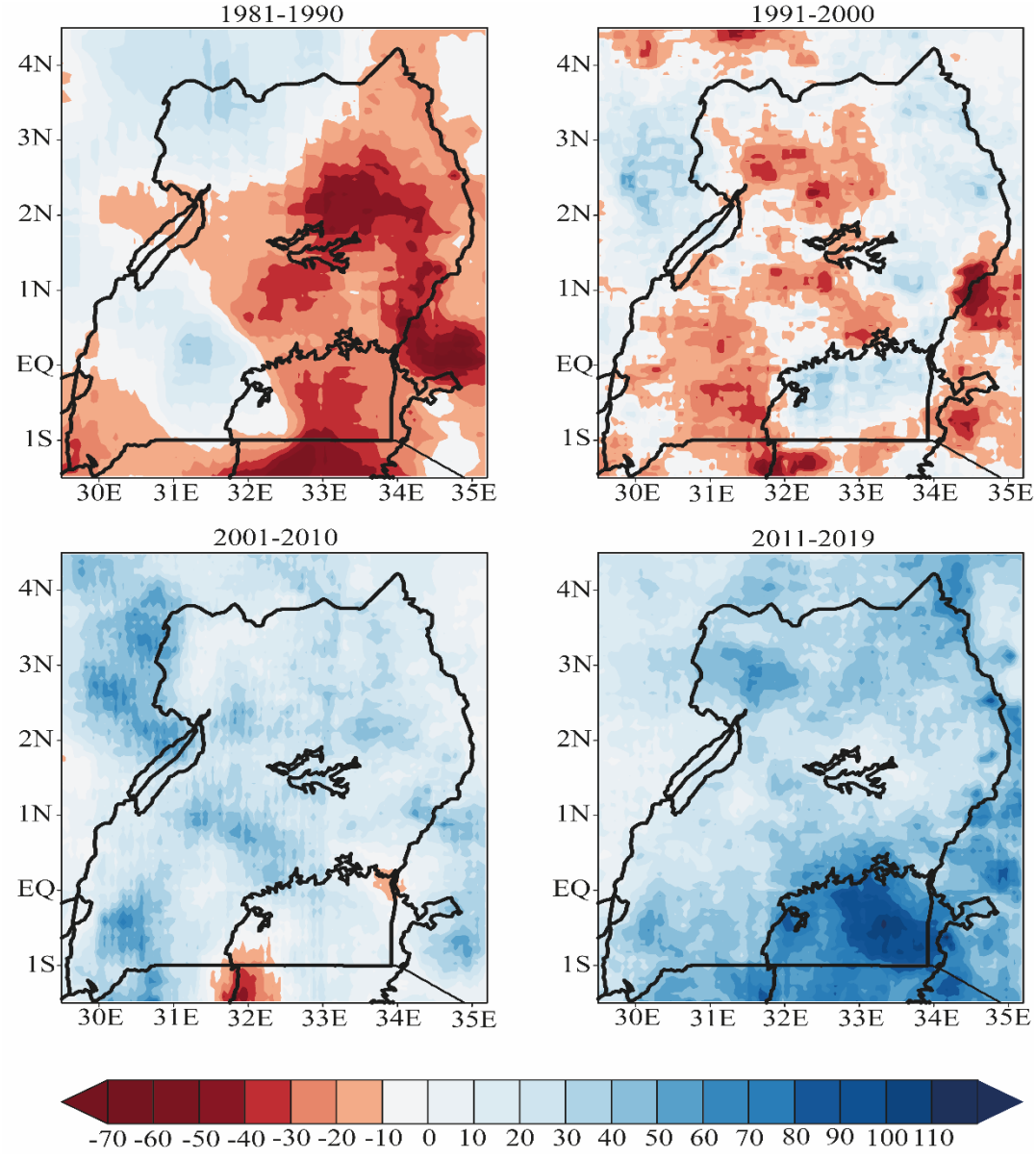


Figure 8. Spatial decadal precipitation anomalies (mm) for SON over Uganda based on CHIRPS.v2 datasets for the period 1981-2019.

*3.4 Historical monotonic trends analysis*

The present study utilized the Mann-Kendall trend test to detect the possible significant and abrupt changes in rainfall patterns over the study area for the given period (1981 – 2019). The results for MAM, annual, and SON time series show Z-score of 0.315, 0.629, and 0.677 (Table 4), which is below the threshold value of 1.96, signifying slight positive tendencies. However, the variance (*S*) shows negative values for all the analysis, indicating a reduction in rainfall for the given period. Figure 8 demonstrates results for sequential Mann-Kendall statistic values of progressive $u$ (t) (solid red line) and retrogressive $u'$ (t) (black dotted line), derived from CHIRPS.v2 precipitation datasets for (a) MAM, (b) SON, and (c) annual mean over Uganda during 1981 – 2019 period. Generally, the SQMK indicates an upward trend in annual and

Preprints (www.preprints.org) | NOT PEER-REVIEWED | Posted: 4 January 2021 doi:10.20944/preprints202101.0037.v1

519 seasonal rainfall over the study area which is indicated using progressive statistic. Essentially,
520 the analysis demonstrates a positive insignificant trend even though the amplitude varies from
521 one season to another. For instance, the MAM season (Figure 9a) showed a decreasing pattern
522 at the start of the study period until 1984 when it experienced noteworthy decrease with a
523 reversed upward trend, experienced thereafter which was eventually sustained until the end of
524 the study period. During this period, change occurred in 2011 as evidenced by the intersection
525 of $u$ (t) and $u'$ (t).

526 On the other hand, the SON season (Figure 9b) experienced several changes, with three
527 major intersections encountered across the study duration. The annual rainfall record presented
528 similar patterns as the MAM season with three changes occurring in 2010, 2013, and 2018
529 where the forward and retrograde line crossed each other (Figure 9c). The results are in
530 congruence with previous findings (Funk et al. 2008; Williams and Funk 2011; Lyon and
531 Dewitt, 2012) that reported an abrupt shift in rainfall tendency from wet years to an almost
532 continuous period well-below average rainfall over the study domain. This trend has been
533 consistent in the three decades, following the early years of 1980s, as well as series of dry years
534 in 2010.

535 Fluctuations in water resources is evident based on the decline in water levels of Lake
536 Victoria mainly as a result of the impact of rainfall variations (Kull 2006). The decreasing trend
537 in MAM total rainfall impacted negatively through a reduction in the number of wet days,
538 thereby affecting the cropping cycle and maturity of staple foods. In some regions, farmers had
539 noticed seasonal rains delayed. Again, they noticed rains received as well as rainfall duration
540 during such periods were short, intensive and erratic. Such scenarios had immense impact on
541 the overall output of food supply and water table. This in effect, calls for implementation of
542 rapid growing crops and systems that required less water as an adaptive mechanism to cope
543 with changes associated with rainfall. Farmers and all relevant stakeholders need to shift the
544 planting season from MAM to SON which currently experiences much rainfall occurrence as
545 compared to MAM.

Preprints (www.preprints.org) | NOT PEER-REVIEWED | Posted: 4 January 2021 doi:10.20944/preprints202101.0037.v1

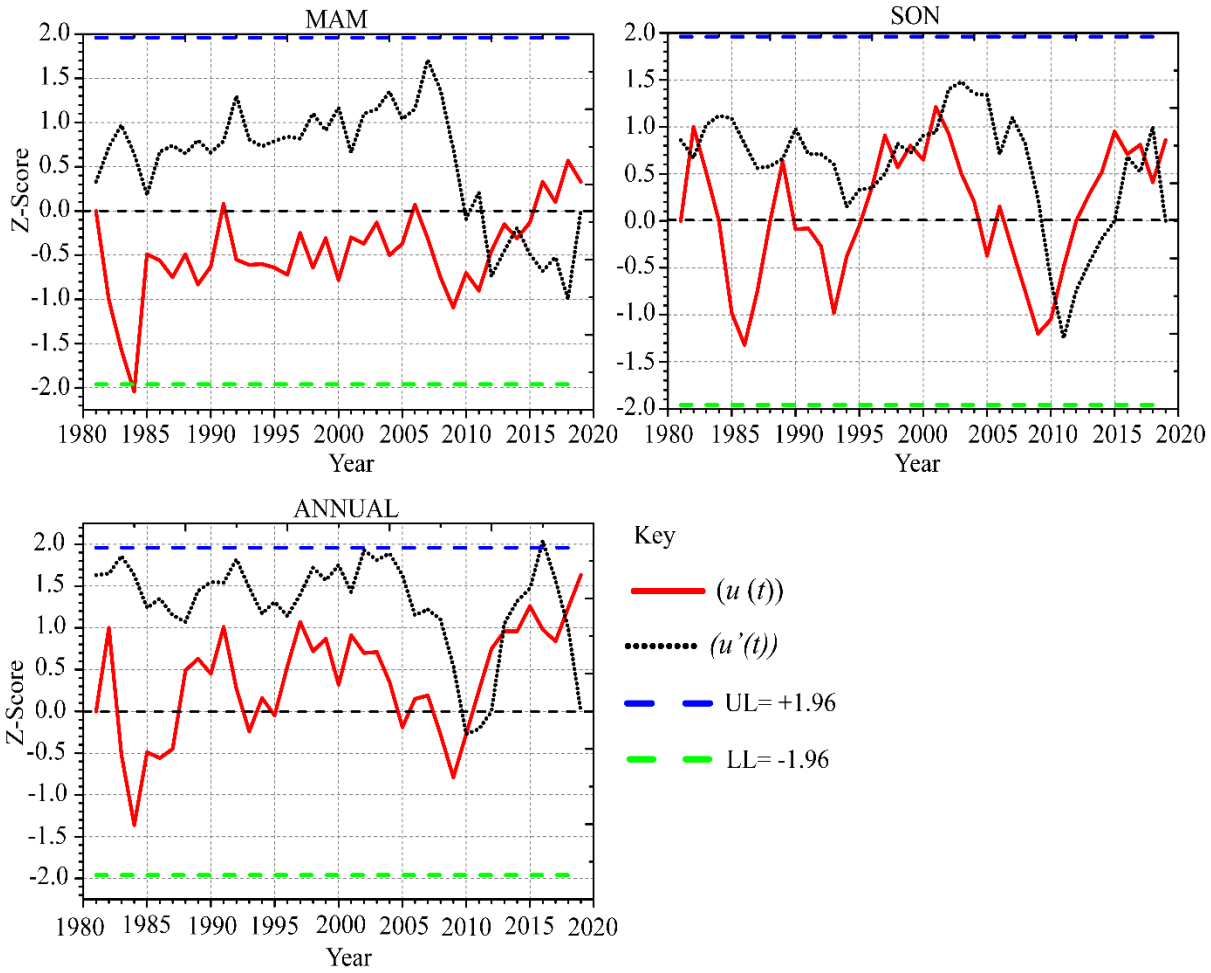


Figure 9. Sequential Mann-Kendall statistic values of progressive u (t) (red solid line) and retrogressive u' (t) (black dotted line), derived from CHIRPS.v2 precipitation datasets for MAM, SON, and Annual mean over Uganda during 1981-2019.

**Table 4.** Summary of Mann-Kendall test statistics for annual, seasonal of MAM and OND rainfall over Uganda at 5% significant level.

| Trend Analysis | | | MK Rainfall (mm) |
|---|---|---|---|
| | Annual_RF | MAM | SON |
| S | -27.00 | -53.00 | -57.00 |
| Z | 0.315 | 0.629 | 0.677 |
| Kendall's tau | 0.182 | 0.0364 | 0.0958 |
| P | 0.753 | 0.529 | 0.498 |
| Alpha $\alpha$ | 0.05 | 0.05 | 0.05 |
| Significance | Insignificant increasing trend | Insignificant decreasing trend | Insignificant decreasing trend |

*3.5 Future Projections*

This study used the MME ensemble to depict the future projections under RCP8.5 in bid to demonstrate the near-term changes in rainfall over the study area. Figure 10 shows the monthly

Preprints (www.preprints.org) | NOT PEER-REVIEWED | Posted: 4 January 2021 doi:10.20944/preprints202101.0037.v1

changes of rainfall in the future for 2020 - 2050 period under RCP8.5, relative to the baseline data for 1981 - 2019 over Uganda. Results show that wet conditions are projected to occur over the study area between April-May and SON season. Contrarily, the month of March is likely to witness a reduction in wet conditions. Projected patterns show further reduction as compared to the baseline period in rainfall during the months of June-August (JJA) and December-February (DJF). Further analysis of projected linear trends of seasonal and annual rainfall over Uganda for the given period (2020 – 2050), relative to 1981-2019 is shown in Figure 11 and Figure 12. The distribution and analysis were to explain projected linear patterns, relative to the baseline period, which highlights the expected changes and their respective magnitude over the study area. Linear trends (Figure 11) and PDF (Figure 12) for seasonal precipitation illustrate decreasing patterns during the long rainy season (Figure 11a & Figure 12a) whilst increasing tendencies with substantial shift is depicted during the SON season (Figure 11b & 12b) over the study region. The resultant implication is an upsurge in rainfall amount received during SON over the study domain. Meanwhile, annual projections (Figure 11c & Figure 12c) indicated huge variations, with linear trends showing a marginal increase as compared to historical tendencies.

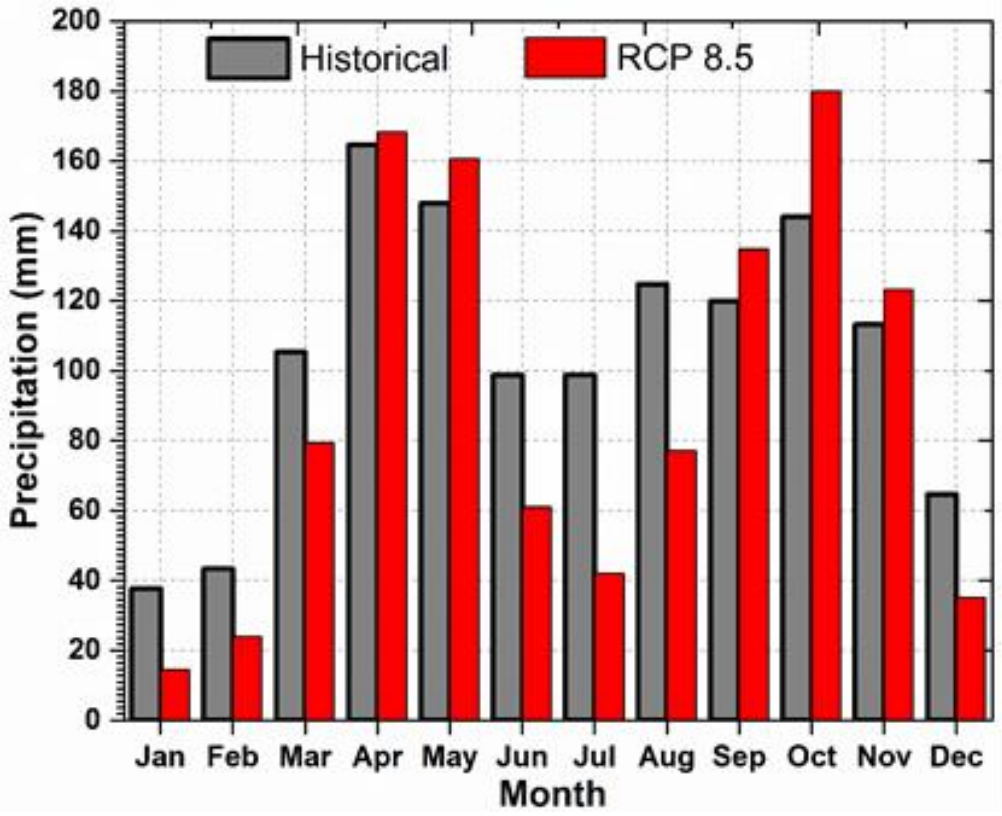


Figure 10. Monthly projected precipitation climatology (mm) for the period 1981-2019 and for the projected period 2020-2050 (mm) over Uganda under RCP 8.5 scenario.

Preprints (www.preprints.org) | NOT PEER-REVIEWED | Posted: 4 January 2021 doi:10.20944/preprints202101.0037.v1

It should be noted that projections were derived from the multi-model ensemble of five better performing RCMs over the study region (Endris et al. 2013; Ayugi et al. 2020a). This was to enhance the confidence in projections due to reduced inter-model uncertainty and minimum biases. The results of the annual cycle (Figure 10) agree with existing studies on projected annual rainfall across the East African (EA) region. For instance, Ongoma et al. (2018) projected an increase in rainfall during the month of April and September while May to August was likely to witness a reduction in wet conditions. The observed and projected dry conditions during JJA could be attributed to changes in above-normal sea-level pressure over Bombay and Indian drought in July through to September, thereby contributing to dry conditions over Uganda, and other parts of EA region (Camberlin 1997; Patricola and Cook 2011).

Nevertheless, the projected wet conditions during the April/May period could be ascribed to strong Somali jet that is southerly over the Horn of Africa and turns westerly into the Arabian Sea, thereby transporting moisture over EA (Hastenrath et al. 2011). The analysis for linear trends as presented in Figure 11 and 12 which depicts negative trends for annual and MAM season could be attributed to reduced rainfall trends during the long rainy season which may account for the higher rainfall amount recorded as compared to the SON season. The projected decrease agrees with recent studies conducted by Rowell et al. (2015) and Tierney et al. (2015) that equally asserted that the projected long rains would continue to exhibit decreasing patterns until 2060 before it depicts recovery trends towards the end of the century. Apparently, other studies demonstrate correspondingly opposite trends over the EA region with increasing patterns being reported contrary to observed reduced trends recorded (Rowell et al. 2015; Ongoma et al. 2018). This discrepancy in projected rainfall trends is termed as the East Africa “climate paradox”. This further calls for more evaluative studies to ascertain clarity in projected patterns (Rowell et al. 2015).

Preprints (www.preprints.org) | NOT PEER-REVIEWED | Posted: 4 January 2021 doi:10.20944/preprints202101.0037.v1

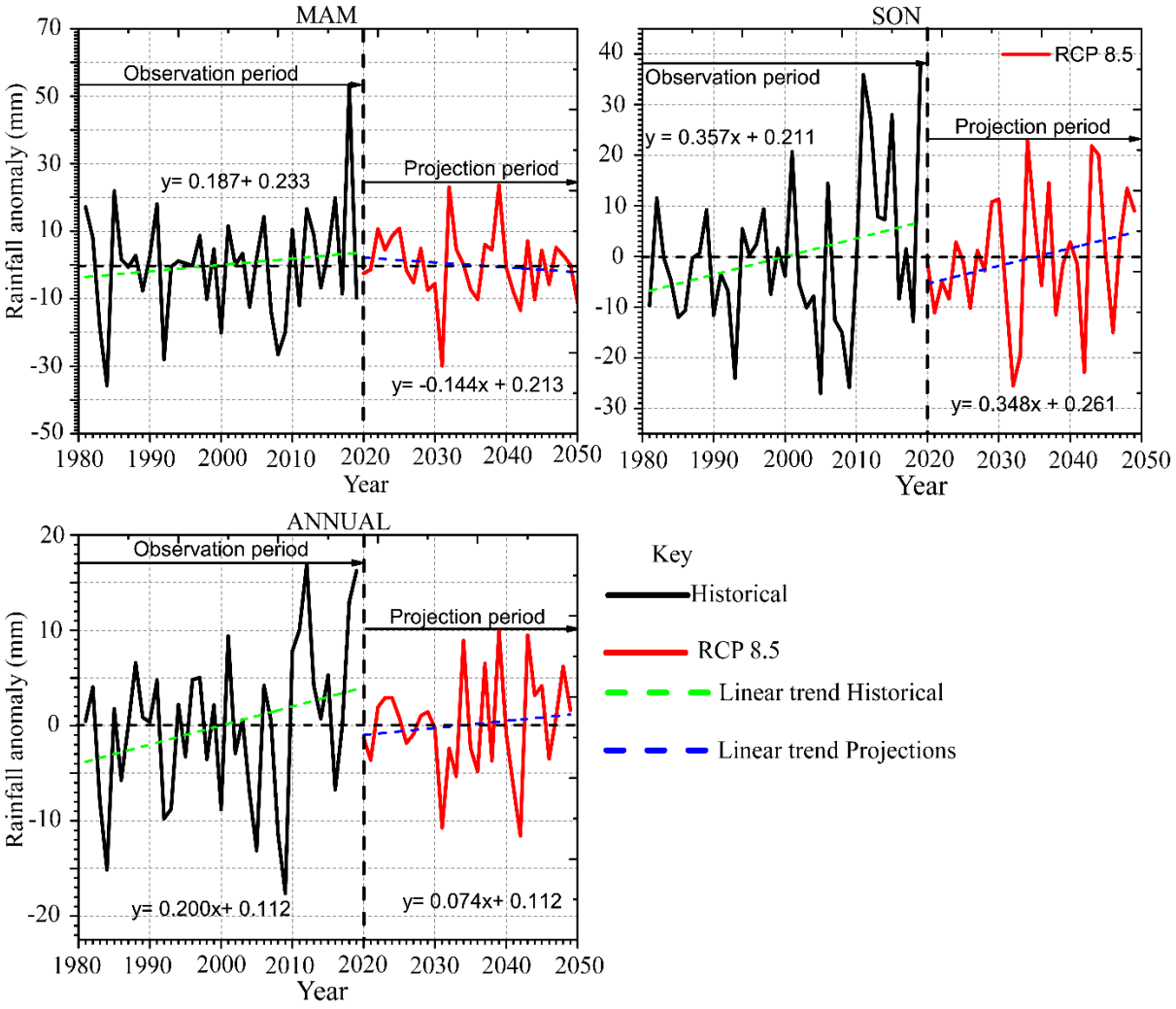


Figure 11. Precipitation anomaly for MAM, SON, and Annual over Uganda under RCP 8.5 for historical simulations based on CHIRPS.v2 during1981-2019 and projections in during 2020-2050 based on five MME RCA4 models

Conversely, the substantial increment in precipitation during SON rains could be attributed to changes in teleconnection patterns such as ENSO and IOD (Nicholson and Kim 1997; Indeje et al. 2000; Endris et al. 2019). These studies illustrated a higher warming rates over the western Indian Ocean than the eastern Indian Ocean. This may lead to intensified positive IOD occurrences, leading to stronger spatial coherence in precipitation patterns. The decisive shift, indicating an increase in rainfall event, despite projected future warming, agrees with a study conducted by Kent et al. (2015) that revealed lack of correlation between uncertainty in global mean temperature and projected end-of-twenty-first-century change in precipitation. Moreover, the study further noted that uncertainty in regional precipitation over the study region is predominantly related to spatial shifts in convection and convergence, associated with processes such as SST patterns and land-sea thermal contrast change. The conclusion in various studies that attempts to elucidate shifts in rainfall projections highlights

 doi:10.20944/preprints202101.0037.v1

the complexity of regional rainfall fluctuations, resulting to uncertainty about the magnitude of impacts, related to extremes weather events. Meanwhile, the projected reductions in rainfall amounts for MAM seasons and annual precipitations could be associated with the weakening of Walker Circulation over Indian and Pacific Ocean basins (Tierney et al. 2015).

In summary, the projected increase in April/May rainfall may be a relief to farmers who entirely depend on rainfall for their agricultural activities. The increased wetness would enhance farm outputs, thereby improving the overall productivity at the national level. However, the projected reduction in JJA rainfall, attributed to Congo westerlies would adversely impact communities, mostly located in southwestern Uganda (Diem et al. 2019a). For instance, the crop regions along the western belt would be affected by the changes in climatic conditions. Further, rapid population growth and an expansion of farming and pastoralism under drier climate regimes would dramatically increase the number of vulnerable communities for the next 30 years. The changes projected could also heighten community conflicts in the use of limited natural resources. Continuous monitoring of rainfall and its related impacts remain a crucial task with short term policies being formulated to reflect the present changes from time to time.

Preprints (www.preprints.org) | NOT PEER-REVIEWED | Posted: 4 January 2021 doi:10.20944/preprints202101.0037.v1

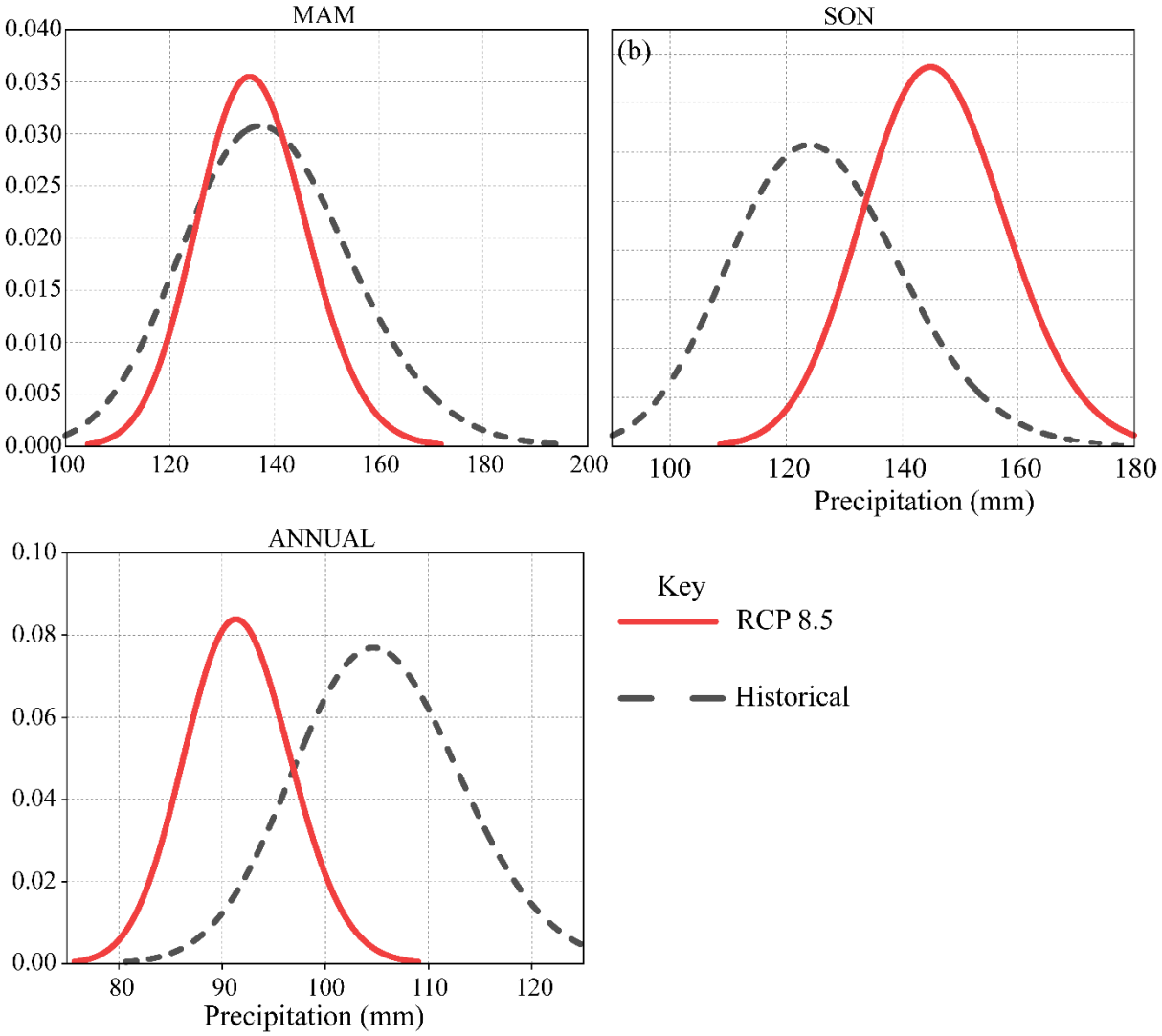


Figure 12. PDF for MAM, SON, and Annual precipitation under RCP 8.5 during 2020-2050 scenarios and baseline period 1981-2019.

## 4. Conclusion and Recommendation

Rainfall remains one of the most important climatic variables supporting the economies and livelihoods of many African countries. Slight variation or changes in its trends translate to massive impact on agriculture, energy, transportation and other climate sensitive sectors of the economy. This present study, thus, sought to examine recent trends and possible future projection of rainfall over Uganda. The study utilized rainfall datasets obtained from Climate Hazard Group Infrared Precipitation with Station (CHIRPS) and multi model ensemble (MME) of five regional climate (RCMs) datasets. The listed RCMs simulations outputs were derived from the dynamical downscaling of CMIP5 GCMs using Rossby Climate Modelling Atmospheric Centre (RCA4), originally developed by the Swedish Meteorological and Hydrological Institute (SMHI) under the CORDEX initiative. The CHIRPS dataset was

646 employed for historical analysis while MME was employed for future projections under
647 RCP8.5 scenario.
648 The results for multi-year monthly climatology show occurrence of bimodal rainfall
649 patterns with strong gradient of rainfall experienced for March-May season (MAM). The
650 second rainfall band on the other hand, occurred in September-November (SON). Results
651 further revealed the study area received less rainfall of < 48 mm/month during December-
652 February season (DJF) while substantial amount of rainfall (107 mm/month) was recorded for
653 the June-August season (JJA). An analysis of recent trends of rainfall revealed an upward trend
654 in annual and seasonal rainfall over study area after 2010. Furthermore, results for future
655 projections show wet conditions are projected to occur over study area between April-May and
656 October. On the contrary, the month of March is likely to witness a reduction in wet conditions
657 based on study findings. Linear trends for seasonal rainfall show decreasing patterns for MAM
658 season whilst increasing tendencies with strong shift are depicted during SON over the study
659 region. Meanwhile, annual projections indicated huge variations with linear trends, illustrating
660 a marginal increase as compared to historical tendencies.
661 The results of this study would contribute to the ever-present debate on projected
662 expected changes in the region's rainfall variation which continues to draw much attention due
663 to the many conflicting projection patterns. The results can be utilized by relevant stakeholders,
664 including policy makers and farmers who largely depends on rainfed climatic patterns in the
665 wake of global warming. Decision and policy makers ought to design
666 appropriate policies that reflect all possible outcomes as various studies are inconclusive on the
667 exact direction of future climate in the wake of global warming and climate change.
668

669 **Acknowledgments**

670 The first author recognizes the support offered by the Ministry of Commerce of the People's
671 Republic of China to pursue graduate studies at Nanjing University of Information Science and
672 Technology (NUIST). Moreover, the infrastructural setup by the University is highly
673 appreciated. All data centers that availed the datasets employed in the present study are
674 acknowledged greatly. The authors are grateful to the anonymous reviewers for the excellent
675 effort and work done which helped in improving the quality of the manuscript.

676 **Compliance with ethical standards**

677 In an undisputed agreement, all authors affirm no conflict of interest in the present study.

678 **References**

679
680 Adhikari U, Nejadhashemi AP, Woznicki SA (2015) Climate change and eastern Africa : a
681 review of impact on major crops. Food Energy Secur 4:110-132.
682 https://doi.org/10.1002/fes3.61
683 Akinsanola AA, Ajayi VO, Adejare AT, Adeyeri OE, Gbode IE, Ogunjobi KO, Nikulin G,
684 Abolude AT (2017) Evaluation of rainfall simulations over West Africa in dynamically
685 downscaled CMIP5 global circulation models. Theor Appl Climatol. DOI:
686 10.1007/s00704-017-2087-8
687 Alex N, Jesse K, Neoline N (2019) Evaluation of past and future extreme rainfall
688 characteristics over Eastern Uganda. Journal of Environmental & Agricultural Sciences.
689 18:38-49.
690 Alexander LV, Zhang X, Peterson TC, Caesar J, Gleason B, Klein Tank AMG, Haylock M,
691 Collins D, Trewin B, Rahimzadeh F, Tagipour A, Rupa Kumar K, Revadekar J, Griffiths
692 G, Vincent L, Stephenson DB, Burn J, Aguilar E, Brunet M, Vazquez-Aguirre JL (2006)
693 Global observed changes in daily climate extremes of temperature and precipitation. J.
694 Geophys. Res 111:D05109. https://doi.org/10.1029/2005JD006290
695 Apuuli B, Wright J, Elias C, Burton I (2000) Reconciling national and global priorities in
696 adaptation to climate change: with an illustration from Uganda. Environmental
697 Monitoring and Assessment 61:145-159.
698 Ayugi BO, Tan G, Ongoma V, Mafuru KB (2018) Circulations Associated with Variations in
699 Boreal Spring Rainfall over Kenya. Earth Syst Environ *2*:421–434.
700 https://doi.org/10.1007/s41748-018-0074-6
701 Ayugi B, Tan G, Gnitou GT, Ojara M, Ongoma V (2020) Historical evaluations and
702 simulations of precipitation over East Africa from Rossby centre regional climate model.
703 Atmos Res 232. https://doi.org/10.1016/j.atmosres.2019.104705
704 Ayugi B, Tan G, Niu R, Dong Z, Ojara M, Mumo L, Babaousmail H, Ongoma V (2020)
705 Evaluation of Meteorological Drought and Flood Scenarios over Kenya, East Africa.
706 Atmosphere 11:307. https://doi.org/10.3390/atmos11030307
707 Ayugi B, Tan G, Ullah W, Boiyo R, Ongoma V (2019) Inter-comparison of remotely sensed
708 precipitation datasets over Kenya during 1998–2016. Atmos Res *225*:96–109.
709 https://doi.org/10.1016/j.atmosres.2019.03.032
710 Basalirwa CPK (1995) Delineation of Uganda into climatological rainfall zones using the
711 method of principal component analysis. Int. J. Climatol 15:1161–1177.
712 https://doi.org/10.1002/joc.3370151008
713 Behera SK, Luo JJ, Masson S, Delecluse P, Gualdi S, Navarra A, Yamagata T (2006) Erratum:
714 Paramount impact of the Indian ocean dipole on the East African short rains: A CGCM J.
715 Climate 18:4514-4530. https://doi.org/10.1175/JCLI3541.1
716 Bowden JH, Semazzi FHM (2007) Empirical Analysis of Intraseasonal Climate Variability
717 over the Greater Horn of Africa. J. Climate 20:5715–5731.
718 https://doi.org/10.1175/2007JCLI1587.1
719 Camberlin P, Wairoto JG (1997) Intraseasonal wind anomalies related to wet and dry spells
720 during the “long” and “short” rainy seasons in Kenya. Theor Appl Climatol 58:57–69.
721 https://doi.org/10.1007/BF00867432
722 Camberlin P (2018) Climate of Eastern Africa. In Oxford Research Encyclopedia of Climate

Science. https://doi.org/10.1093/acrefore/9780190228620.013.512

Chai T, Draxler RR (2014) Root mean square error (RMSE) or mean absolute error (MAE)? – Arguments against avoiding RMSE in the literature. Geo Sci. Model Dev 7:1247–1250. https://doi.org/10.5194/gmd-7-1247-2014

Christensen J H, Boberg F, Christensen OB, Lucas PP (2008) On the need for bias correction of regional climate change projections of temperature and precipitation, Geophys. Res. Lett., 35, L20709, https://doi.org/10.1029/2008GL035694.

Christensen JH, Krishna Kumar K, Aldrian E, An SI, Cavalcanti IFA, de Castro M, Dong W, Goswami P, Hall A, Kanyanga JK, Kitoh A, Kossin J, Lau N-C, Renwick J, Stephenson DB, Xie S-P, Zhou T (2011) Climate Phenomena and their Relevance for Future Regional Climate Change. In Intergovernmental Panel on Climate Change (Ed.), *Climate Change 2013* - The Physical Science Basis 1217–1308. Cambridge University Press. https://doi.org/10.1017/CBO9781107415324.028

Diem JE, Hartter J, Ryan SJ, Palace MW (2014) Validation of satellite rainfall products for Western Uganda. J. Hydrometeorol 15:2030–2038. https://doi.org/10.1175/JHM-D-13-0193.1

Diem JE, Sung HS, Konecky BL, Palace MW, Salerno J, Hartter J (2019) Rainfall Characteristics and Trends—and the Role of Congo Westerlies—in the Western Uganda Transition Zone of Equatorial Africa From 1983 to 2017. J. Geophys. Res 124:10712–10729. https://doi.org/10.1029/2019JD031243

Diem JE, Konecky BL, Salerno J, Hartter J (2019) Is equatorial Africa getting wetter or drier? Insights from an evaluation of long-term, satellite-based rainfall estimates for western Uganda. Int J Climatol. 1–14. https://doi.org/10.1002/joc.6023

Dufresne JL, Foujols MA, Denvil S, Caubel A, Marti O (2012) Climate change projections using the IPSL-CM5 earth system model: from CMIP3 to CMIP5. Clim Dyn. doi:10.1007/s00382-012-1636-1

Eckstein D, Künzel V, Schäfer L, Winges M (2020) Global Climate Risk Index 2020. Bonn: Germanwatch.

Endris HS, Lennard C, Hewitson B, Dosio A, Nikulin G, Artan GA (2019) Future changes in rainfall associated with ENSO, IOD and changes in the mean state over Eastern Africa. Clim dynm 52:2029–2053. https://doi.org/10.1007/s00382-018-4239-7

Endris HS, Omondi P, Jain S, Lennard C, Hewitson B, Chang'a L, Awange JL, Dosio A, Ketiem P, Nikulin G, Panitz HJ, Büchner M, Stordal F, Tazalika L (2013) Assessment of the performance of CORDEX regional climate models in simulating East African rainfall. J. Climate 26:8453–8475. https://doi.org/10.1175/JCLI-D-12-00708.1

Eyring V, Cox PM, Flato GM, Gleckler PJ , Gab Abramowitz G, Caldwell P , Collins WD, Gier BK, Alex D. Hall AD , Hoffman FM, Hurtt GC, Jahn A, Jones CD, Klein SA, Krasting JP, Kwiatkowski L, Lorenz R, Maloney E, Meehl GA, Pendergrass AG, Pincus R, Ruane AC, Russell JL, Sanderson BM, Santer BD, Sherwood SC, Simpson IR, Stouffer RJ, Williamson MS (2019) Taking climate model evaluation to the next level. *Nature Clim Change* 9**:** 102–110 https://doi.org/10.1038/s41558-018-0355-y

FAO (2013) Technical note : Analysis of price incentives for rice in Uganda for the time period 2005 - 2013 Rome, Italy

FAO, IFAD, UNICEF, WFP, WHO (2017) The State of Food Security and Nutrition in the World. Building resilience for peace and food security. Rome, FAO.

Funk C, Dettinger MD, Michaelsen JC, Verdin JP, Brown ME, Barlow M, Hoell A (2008) Warming of the Indian Ocean threatens eastern and southern African food security but could be mitigated by agricultural development. PNAS 105:11081–11086. https://doi.org/10.1073/pnas.0708196105

Funk C, Peterson P, Landsfeld M, Pedreros D, Verdin J, Shukla S, Husak G, Rowland J, Harrison L, Hoell A, Michaelsen J (2015) The climate hazards infrared precipitation with stations - A new environmental record for monitoring extremes. Scientific Data 2: 1–21. https://doi.org/10.1038/sdata.2015.66

Funk JL, Jones CG, Gray DW, Throop HL, Hyatt LA, Lerdau MT (2005) Variation in isoprene emission from Quercus rubra: Sources, causes, and consequences for estimating fluxes**.** J Geophys Res Atmos 110: 1–10. https://doi.org/10.1029/2004JD005229

Gamoyo M, Reason C, Obura D (2015) Rainfall variability over the East African coast. Theor appl climatol 120:311–322. https://doi.org/10.1007/s00704-014-1171-6

Gebrechorkos SH, Hülsmann S, Bernhofer C (2017) Evaluation of Multiple Climate Data Sources for Managing Environmental Resources in East Africa. Hydrol. Earth Syst. Sci 22:4547-4564 https://doi.org/10.5194/hess-2017-558

Giannini A, Saravanan R, Chang P (2005) Dynamics of the boreal summer African monsoon in the NSIPP1 atmospheric model. Clim dynm 25:517-535. DOI 10.1007/s00382-005-0056-x

Gilbert RO (1987) Statistical Methods for Environmental Pollution Monitoring. John Wiley & Sons.

Giorgi F, Gutowski WJ (2015) Regional Dynamical Downscaling and the CORDEX Initiative. Annu Rev Environ Resour 40: 467–490. https://doi.org/10.1146/annurev-environ-102014-021217

Gollin D, Jedwab R, Vollrath D (2016) Urbanization with and without industrialization. **J** Econ Growth 21:35–70. https://doi.org/10.1007/s10887-015-9121-4

Government of Uganda (GOU) (2015) Economic Assessment of the Impacts of Climate Change in Uganda. Final Study Report. Ministry of Water and Environment, Climate Change Department Kampala.

Hastenrath S, Polzin D, Mutai C (2011) Circulation mechanisms of kenya rainfall anomalies. J. Climate 24:404–412. https://doi.org/10.1175/2010JCLI3599.1

Hazeleger W, Wang X, Severijns C, S¸tefa˘nescu S, Bintanja R, Sterl A, Wyser K, Semmler T, Yang S, van den Hurk B, van Noije T, van der Linden E, van der Wiel K (2012) EC-Earth V2.2: description and validation of a new seamless earth system prediction model. Clim Dyn 39:2611–2629 DOI 10.1007/s00382-011-1228-5

Hession S L, Moore N (2011) A spatial regression analysis of the influence of topography on monthly rainfall in East Africa. Int. J. Climatol 31:1440–1456. https://doi.org/10.1002/joc.2174

Hollander M, Wolfe DA, Chicken E (2013) Nonparametric Statistical Methods, vol. 751. John Wiley & Sons

Indeje M, Semazzi FHM, Xie L, Ogallo LJ (2001) Mechanistic model simulations of the East African climate using NCAR regional climate model: Influence of large-scale orography

on the Turkana low-level jet. J. Climate 14:2710–2724. https://doi.org/10.1175/1520-0442(2001)014<2710:MMSOTE>2.0.CO;2

Indeje M, Semazzi FHM, Ogallo LJ (2000) ENSO signals in East African rainfall seasons. Int. J. Climatol 20:19–46. https://doi.org/10.1002/(SICI)1097-0088(200001)20:1<19::AID-JOC449>3.0.CO;2-0

IPCC (2014) Climate Change 2014: Synthesis Report. Contribution of Working Groups I, II and III to the Fifth Assessment Report of the Intergovernmental Panel on Climate Change [Pachauri RK, Meyer LA (eds.)]. IPCC, Geneva, Switzerland, 151 pp.

IPCC (2013) Climate Change 2013: The Physical Science Basis. Contribution of Working Group I to the Fifth Assessment Report of the Intergovernmental Panel on Climate Change [Stocker TF, Qin D, Plattner G-K, Tignor M, Allen SK, Boschung J, Nauels A, Xia Y, Bex V, Midgley PM (eds.)]. Cambridge University Press, Cambridge, United Kingdom and New York, NY, USA, 1535 pp.

IPCC (2001) Climate Change 2001: The Scientific Basis, Contribution of Working Group I to the Third Assessment Report of the Intergovernmental Panel on Climate Change (Houghton JT, Ding Y, Griggs DJ, Noguer M, van der Linden PJ, Dai X, Maskell K, Johnson CA (eds.)]. Cambridge University Press, Cambridge, United Kingdom and New York, NY, USA, 881 pp. (see http://www.grida.no/climate/ipcc_tar/wg1/317.htm#fig84)

Kendall MG (1975) Rank correlation methods, 4th edn. Griffin, London, p 202

Kent C, Chadwick R, Rowell,DP (2015) Understanding uncertainties in future projections of seasonal tropical precipitation. J. Climate 28:4390–4413. https://doi.org/10.1175/JCLI-D-14-00613.1

Kidd C, Bauer P, Turk J, Huffman GJ, Joyce R, Hsu KL, Braithwaite D (2012) Intercomparison of high-resolution precipitation products over Northwest Europe. J. Hydrometeorol 13:67–83. https://doi.org/10.1175/JHM-D-11-042.1

Kimani MW, Hoedjes JCB, Su Z (2017) An assessment of satellite-derived rainfall products relative to ground observations over East Africa. Remote Sens 9: https://doi.org/10.3390/rs9050430

Kisembe J, Favre A, Dosio A, Lennard,C, Sabiiti G, Nimusiima A (2019) Evaluation of rainfall simulations over Uganda in CORDEX regional climate models. Theor appl climatol 137:1117–1134. https://doi.org/10.1007/s00704-018-2643-x

Kizza M, Rodhe A, Xu CY, Ntale HK, Halldin S (2009) Temporal rainfall variability in the Lake Victoria Basin in East Africa during the twentieth century. Theor appl climatol 98: 119–135. https://doi.org/10.1007/s00704-008-0093-6

Kull D (2006) Connections between recent water level drops in Lake Victoria, dam operations and drought. available at: www.irn.org/programs/nile/pdf/060208vic.pdf (accessed 24 March 2013).

Liebmann B, Hoerling MP, Funk C, Bladé I, Dole RM, Allured D, Quan X, Pegion P, Eischeid JK (2014) Understanding recent eastern Horn of Africa rainfall variability and change. Int. J. Climatol 27: 8630–8645. https://doi.org/10.1175/JCLI-D-13-00714.1

Lyon B, Dewitt DG (2012) A recent and abrupt decline in the East African long rains. Geophys. Res. Lett 39:1–5. https://doi.org/10.1029/2011GL050337

MacLeod D (2019) Seasonal forecasts of the East African long rains: insight from atmospheric relaxation experiments. Clim dynm 53:4505–4520. https://doi.org/10.1007/s00382-019-

04800-6
Makkonen L (2006) Plotting Positions in Extreme Value Analysis. J Clim Appl Meteorol 45: 334–340.
Manatsa D, Chipindu B, Behera SK (2012) Shifts in IOD and their impacts on association with East Africa rainfall**.** Theor appl climatol *110*: 115–128. https://doi.org/10.1007/s00704-012-0610-5
Mann HB (1945) Nonparametric tests against trend. Econometrica 13:245–259
Matthew OJ, Abiodun BJ, Salami AT (2015) Modelling the impacts of climate variability on crop yields in Nigeria: Performance evaluation of RegCM3-GLAM system. Meteorol. Appl 22: 198–212. https://doi.org/10.1002/met.1443
Mchugh MJ (2004) Near-Surface Zonal Flow and East African Precipitation Receipt during Austral Summer. J. Clim 17 4070–4079. https://doi.org/10.1175/1520-0442(2004)017<4070:NZFAEA>2.0.CO;2
McSweeney C, New M, Lizcano G, Lu X (2010) The UNDP climate change country profiles. Bull. Am. Meteorol. Soc 91:157–166. https://doi.org/10.1175/2009BAMS2826.1
Mutai CC, Ward MN (2000) East African rainfall and the tropical circulation/convection on intraseasonal to interannual timescales. J. Climate 13: 3915–3939. https://doi.org/10.1175/1520-0442(2000)013<3915:EARATT>2.0.CO;2
Muhati FD, Ininda JM, Opijah FJ (2007) Relationship between ENSO parameters and the trends and periodic flactuations in east African rainfall. J Kenya Meteorol Soc 1: 20–43.
Mumo L, Yu J, Ayugi B (2019) Evaluation of spatiotemporal variability of rainfall over Kenya from 1979 to 2017. J. Atmos. Sol. Terr. Phys. 105097.
Niang I, Ruppel OC, Abdrabo MA, Essel A, Lennard C, Padgham J, Urquhart P (2014) Africa. In: *Climate Change 2014: Impacts, Adaptation, and Vulnerability. Part B: Regional Aspects. Contribution of Working Group II to the Fifth Assessment Report of the Intergovernmental Panel on Climate Change* [Barros VR, Field CB, Dokken DJ, Mastrandrea MD, Mach KJ, Bilir TE, Chatterjee M, Ebi KL, Estrada YO, Genova RC, Girma B, Kissel ES, Levy AN, MacCracken S, Mastrandrea PR, White LL (eds.)]. Cambridge University Press, Cambridge, United Kingdom and New York, NY, USA, 1199–1265 pp.
Nicholson SE, Klotter D, Zhou L, Hua W (2019) Validation of satellite precipitation estimates over the Congo Basin. J. Hydrometeorol *20*: 631–656. https://doi.org/10.1175/JHM-D-18-0118.1
Nicholson SE (2018) The ITCZ and the Seasonal Cycle over Equatorial Africa. Bull. Amer. Meteor. Soc. 99 (2): 337–348. https://doi.org/10.1175/BAMS-D-16-0287.1
Nicholson SE, Funk C, Fink A H (2018) Rainfall over the African continent from the 19th through the 21st century. Global Planet. Change 165:114–127. https://doi.org/10.1016/j.gloplacha.2017.12.014
Nicholson SE (2017) Climate and climatic variability of rainfall over eastern Africa. Rev. Geophys. 55, 590–635. doi:10.1002/2016RG000544.
Nicholson SE, Kim J (1997) The relationship of the El Niño–Southern Oscillation to African rainfall. Int. J. Climatol 17:117–135. https://doi.org/10.1002/(SICI)1097-0088(199702)17:2<117::AID-JOC84>3.0.CO;2-O

899 Nikulin G, Jones C, Giorgi F, Asrar G, Büchner M, Cerezo-Mota R, Christensen OB, Déqué
900 M, Fernandez J, Hänsler A, van Meijgaard E, Samuelsson P, Sylla MB, Sushama L (2012)
901 Precipitation climatology in an ensemble of CORDEX-Africa regional climate
902 simulations. J. Climate 25:6057–6078. https://doi.org/10.1175/JCLI-D-11-00375.1
903 Nsubuga FNW, Rautenbach H (2017) Climate change and variability: a review of what is
904 known and ought to be known for Uganda. Int. J Clim Chang Str. 10(5): 752-771 DOI
905 10.1108/IJCCSM-04-2017-0090
906 Nsubuga FNW, Olwoch JM, de Rautenbach CJW, Botai OJ (2014) Analysis of mid-twentieth
907 century rainfall trends and variability over southwestern Uganda. Theor appl climatol
908 115:53–71. https://doi.org/10.1007/s00704-013-0864-6
909 Nsubuga FWN, Olwoch JM, Rautenbach CJdeW (2011) Climatic trends at Namulonge in
910 Uganda: 1947-2009. Journal of Geography and Geology, Vol. 3 No. 1, pp. 119-131.
911 Ntale HK, Gan TY (2003) Drought indices and their application to East Africa. Int. J. Climatol
912 23: 1335–1357. https://doi.org/10.1002/joc.931
913 Ogwang BA, Chen H, Li X, Gao C (2014) The influence of topography on East African
914 October to December climate: Sensitivity experiments with RegCM4. *Adv. Meteorol*
915 https://doi.org/10.1155/2014/143917
916 Ogwang BA, Ongoma V, Xing L, Ogou FK (2015) Influence of mascarene high and Indian
917 Ocean dipole on East African extreme weather events. Geogr. Pannonica 19:64–72.
918 https://doi.org/10.5937/geopan1502064o
919 Ojara MA, Lou Y, Aribo L, Namumbya S, Uddin MJ (2020) Dry spells and probability of
920 rainfall occurrence for Lake Kyoga Basin in Uganda, East Africa. *Nat Hazards* 100**:** 493–
921 514. https://doi.org/10.1007/s11069-019-03822-x
922 Omondi PA, Awange JL, Forootan E, Ogallo LA., Barakiza R, Girmaw GB, Fesseha I,
923 Kululetera V, Kilembe C, Mbati MM, Kilavi M, King'uyu SM, Omeny PA, Njogu A,
924 Badr EM, Musa TA, Muchiri P, Bamanya D, Komutunga E (2014) Changes in
925 temperature and precipitation extremes over the Greater Horn of Africa region from 1961
926 to 2010. Int. J. Climatol 34:1262–1277. https://doi.org/10.1002/joc.3763
927 Ongoma V, Rahman MA, AyugI B, Nisha F, Galvin S, Shilenje ZW, Ogwang BA (2020)
928 Variability of diurnal temperature range over Pacific Island countries,
929 a case study of Fiji. Meteorol atmos phys https://doi.org/10.1007/s00703-020-00743-4
930 Ongoma V, Chen H (2017) Temporal and spatial variability of temperature and precipitation
931 over East Africa from 1951 to 2010. Meteorol atmos phys *129*:131–144.
932 https://doi.org/10.1007/s00703-016-0462-0
933 Ongoma V, Chena H, Gaoa C (2018) Projected changes in mean rainfall and temperature over
934 east Africa based on CMIP5 models. Int. J. Climatol 38:1375–1392.
935 https://doi.org/10.1002/joc.5252
936 Osima S, Indasi VS, Zaroug M, Endris HS, Gudoshava M, Misiani HO, Nimusiima A, Anyah
937 RO, Otieno G, Ogwang BA, Jain S, Kondowe AL, Mwangi E, Lennard C, Nikulin G,
938 Dosio A (2018) Projected climate over the Greater Horn of Africa under 1.5 °C and 2 °C
939 global warming. Environ. Res. Lett *13*:065004. https://doi.org/10.1088/1748-
940 9326/aaba1b
941 Patricola CM, Cook KH (2011) Sub-Saharan Northern African climate at the end of the twenty-
942 first century: Forcing factors and climate change processes. Clim dynm 37:1165–1188.

https://doi.org/10.1007/s00382-010-0907-y

Parry M, Rosenzweig C, Livermore M (2005) Climate change, global food supply and risk of hunger. *Philos. Trans. R. Soc. B Biol. Sci* 360:2125–2138. https://doi.org/10.1098/rstb.2005.1751

Raddatz TJ, Reick CH, Knorr W, Kattge J, Roeckner E, Schnur R, Schnitzler KG, Wetzel P, Jungclaus J (2007) Will the tropical land biosphere dominate the climate-carbon cycle feedback during the twenty-first century? Clim Dyn 29(6):565–574

Reliefweb (2020) East Africa: Drought. 2014-2019. Available at: https://reliefweb.int/disaster/dr-2014-000131-ken. Last accessed on 01 September 2020

Riahi K, Grüble A, Nakicenovic N (2007) Scenarios of long-term socio-economic and environmental development under climate stabilization. Technol Forecast Soc Change. 74(7): 887-935 https://doi.org/10.1016/j.techfore.2006.05.026

Rotstayn LD, Collier MA, Dix MR, Feng Y, Gordon HB, O'Farrell SP, Smith IN, Syktus J (2009) Improved simulation of Australian climate and ENSO-related climate variability in a GCM with an interactive aerosol treatment. Int J Climatol 30:1067–1088

Rowell DP, Booth BBB, Nicholson SE, Good P (2015) Reconciling past and future rainfall trends over East Africa. J. Climate 28:9768–9788. https://doi.org/10.1175/JCLI-D-15-0140.1

Saji NH, Goswami BN, Vinayachandran PN, Yamagata T (1999) A dipole mode in the tropical Indian ocean. Nature 401: 360–363. https://doi.org/10.1038/43854

Saji NH, Yamagata T (2003) Structure of SST and surface wind variability during Indian Ocean Dipole mode events: COADS observations. J. Climate 16: 2735–2751. https://doi.org/10.1175/1520-0442(2003)016<2735:SOSASW>2.0.CO;2

Schlenker W, Lobell DB (2010) Robust negative impacts of climate change on African agriculture. Environ. Res. Lett *5*: 014010. https://doi.org/10.1088/1748-9326/5/1/014010

Sen PK (1968) Estimates of the regression coefficient based on Kendall's tau. J. Am. Stat. Assoc. 63, 1379–1389. https://doi.org/10.2307/2285891.

Seneviratne SI, Wilhelm M, Stanelle T, Van Den Hurk B, Hagemann S, Berg A, Cheruy F, Higgins ME, Meier A, Brovkin V, Claussen M, Ducharne A, Dufresne JL, Findell KL., Ghattas J, Lawrence DM, Malyshev S, Rummukainen M, Smith B (2013) Impact of soil moisture-climate feedbacks on CMIP5 projections: First results from the GLACE-CMIP5 experiment. Geophys. Res**. Lett** *40*:5212–5217. https://doi.org/10.1002/grl.50956

Seneviratne SI, Nicholls N, Easterling D, Goodess CM, Kanae S, Kossin J, Luo Y, Marengo J, McInnes K, Rahimi M, Reichstein M, Sorteberg A, Vera C, Zhang X (2012) Changes in climate extremes and their impacts on the natural physical environment. In: Field CB, Barros V, Stocker TF, Qin D, Dokken DJ, Ebi KL, Mastrandrea MD, Mach KJ, Plattner G-K, Allen SK, Tignor M, Midgley PM (eds) Managing the risks of extreme events and disasters to advance climate change adaptation. A special report of working groups I and II of the intergovernmental panel on climate change. Cambridge University Press, Cambridge, pp 109–230

Sillmann J, Kharin VV, Zhang X, Zwiers FW, Bronaugh D (2013) Climate extremes indices in the CMIP5 multimodel ensemble: Part 1. Model evaluation in the present climate**.** *J*

Geophys Res Atmos *118*: 1716–1733. https://doi.org/10.1002/jgrd.50203

Sneyers R (1990) On the Statistical Analysis of a Series of Observations. Tech Note 143: WMO-No. 415, 192

Spinage CA (2012) African ecology - Benchmarks and historical perspectives. In *African Ecology - Benchmarks and Historical Perspectives*. https://doi.org/10.1007/978-3-642-22872-8

Samuelsson P, Jones CG, Willén U, Ullerstig A, Gollvik S, Hansson U, Jansson C, Kjellströ E, Nikulin G, Wyser K (2012) The Rossby Centre regional climate model RCA3: model description and performance. *Tellus A* 63:4–23. https://doi:10.1111/j.1600-0870.2010.00478.x

Ssentongo P, Muwanguzi AJB, Eden U, Sauer T, Bwanga G, Kateregga G, Aribo L, Ojara M, Mugerwa WK, Schiff SJ (2018) Changes in Ugandan Climate Rainfall at the Village and Forest Level. Sci. Rep 8:3551. https://doi.org/10.1038/s41598-018-21427-5

Strandberg G, Bärring L, Hansson U, Jansson C, Jones C, Kjellström E, Michael K, Marco KG, Nikulin PS., Wang AUS (2014) CORDEX scenarios for Europe from the Rossby Centre regional climate model RCA4. *Rep. Meteorol. Climatol 116*:1–84. https://www.smhi.se/polopoly_fs/1.90273!/Menu/general/extGroup/attachmentColHold/mainCol1/file/RMK_116.pdf

Taylor KE (2001) in a Single Diagram. J. Geophys. Res *106*:7183–7192. https://doi.org/10.1029/2000JD900719

Teutschbein C, Seibert J (2010) Regional climate models for hydrological impact studies at the catchment scale: a review of recent modeling strategies. Geogr.Comp, 4(7), 834-860. doi:10.1111/j.1749-8198.2010.00357.x

Teutschbein C, Seibert J (2013) Is bias correction of regional climate model (RCM) simulations possible for non-stationary conditions?. Hydrol. Earth Syst. Sci, *17*(12), 5061-5077. doi:10.51194/hess-17-5061-2013

Tian Y, Peters-Lidard CD, Adler RF, Kubota T, Ushio T (2010) Evaluation of GSMaP precipitation estimates over the contiguous United States. J. Hydrometeorol *11*: 566–574. https://doi.org/10.1175/2009JHM1190.1

Tierney JE, Ummenhofer CC, DeMenocal PB (2015) Past and future rainfall in the Horn of Africa. Sci. Adv *1*:1–9. https://doi.org/10.1126/sciadv.1500682

Toté C, Patricio D, Boogaard H, van der Wijngaart R, Tarnavsky E, Funk C (2015) Evaluation of satellite rainfall estimates for drought and flood monitoring in Mozambique. Remote Sens 7:1758–1776. https://doi.org/10.3390/rs70201758

Unden P, Rontu L, Jinen H, Lynch P, Calvo J, Cats G, Cuxart J, Eerola K, Fortelius C, Garcia-Moya JA, Jones C, Geert Lenderlink G, Mcdonald A, Mcgrath R, Navascues B, Nielsen NW, Degaard V, Rodriguez E, Rummukainen M, Sattler K, Sass BH, Savijarvi H, Schreur BW, Sigg R (2002) HIRLAM-5 Scientific Documentation. https://repositorio.aemet.es/bitstream/20.500.11765/6323/1/HIRLAMSciDoc_Dec2002.pdf (Accessed 20 Feb 2020)

Vellinga M, Milton SF (2018) Drivers of interannual variability of the East African "Long Rains." *Q J ROY METEOR SOC 144*:861–876. https://doi.org/10.1002/qj.3263

Veronika E, Peter MC, Gregory MF, Peter JG, Gab A, Peter C, William D Collins, Bettina KG, Alex DH, Forrest MH, George CH, Alexandra J, Chris DJ, Stephen AK, John PK,

Lester K, Ruth L, Eric M, Gerald AM, Angeline GP, Robert P, Alex CR, Joellen LR, Benjamin MS, Benjamin DS, Steven CS, Isla RS, Ronald JS Mark SW (2019) Taking climate model evaluation to the next level. Nat Clim Chang 9: 102-110 https://doi.org/10.1038/s41558-018-0355-y

Wang G, Gong T, Lu J, Lou D, Hagan D F T, Chen T (2018) On the long-term changes of drought over China (1948–2012) from different methods of potential evapotranspiration estimations. Int. J. Climatol, 38, 2954–2966. https://doi.org/10.1002/joc.5475

Watanabe S, Hajima T, Sudo K, Nagashima T, Takemura T, Okajima H, Nozawa T, Kawase H, Abe M, Yokohata T, Ise T, Sato H, Kato E, Takata K, Emori S, Kawamiya M (2011) MIROC-ESM 2010: model description and basic results of CMIP5- 20c3 m experiments. GMD 4(4):845–872

White WB, Tourre YM (2003) Global SST/SLP waves during the 20th century. Geophys. Res. Lett, 30: 1651 doi:10.1029/2003GL017055

Wilks SD (2006) Statistical methods in the Atmospheric Science.2nd Edn. Academic Press

Williams AP, Funk C (2011) A westward extension of the warm pool leads to a westward extension of the Walker circulation, drying eastern Africa. Clim dyn 37: 2417–2435. https://doi.org/10.1007/s00382-010-0984-y

Yang W, Seager R, Cane MA, Lyon B (2015) The rainfall annual cycle bias over East Africa in CMIP5 coupled climate models. J. Climate *28*:9789–9802. https://doi.org/10.1175/JCLI-D-15-0323.1

Yin X, Nicholson SE (2002) Interpreting Annual Rainfall from the Levels of Lake Victoria. J. Hydrometeorol *3*: 406–416. https://doi.org/10.1175/1525-7541(2002)003<0406:IARFTL>2.0.CO;2